

Dorsa Kabiri

On the Cell-to-Cell Extracellular Vesicle Transmission within the Brain

Case Study: Alzheimer's Disease

Master's thesis in Electronic Systems Design

Supervisor: Mladen Veletić

Co-supervisor: Martin Damrath, Ilanko Balasingham

July 2023

Dorsa Kabiri

On the Cell-to-Cell Extracellular Vesicle Transmission within the Brain

Case Study: Alzheimer's Disease

Master's thesis in Electronic Systems Design
Supervisor: Mladen Veletić
Co-supervisor: Martin Damrath, Ilanko Balasingham
July 2023

Norwegian University of Science and Technology
Faculty of Information Technology and Electrical Engineering
Department of Electronic Systems



Norwegian University of
Science and Technology

Abstract

Extracellular vesicles are small structures released by cells and play an important role in molecular communication between cells. Each cell in the body acts as a sender and receiver of extracellular vesicles. Because these vesicles carry important biological information, they have great potential for medical applications such as diagnosis and therapy.

In this thesis, extracellular vesicle-mediated communication in the brain is studied in the context of early detection of Alzheimer's disease. Alzheimer's disease is a significant health concern due to its profound impact on individuals, families, and society. It is particularly challenging because the diagnosis often occurs at a late stage, limiting the effectiveness of available treatments. Early diagnosis can help the patients and their families to be better prepared and have more time to make better decisions for future cures and life plans.

A point-to-point communication theoretical model for extracellular transfer between cells is thus established. Specifically, neurons are considered as the transmitter and receiver of a communication system, and the extracellular matrix of the brain is considered as the propagation channel. Moreover, the effects of Alzheimer's disease on the defined link are studied, assuming that the performance of the communication link can serve as a biomarker of the development of the disease and help in its earlier diagnosis.

Sammendrag

Ekstracellulære vesikler er små strukturer som frigjøres av celler og spiller en viktig rolle i cellekommunikasjon. Hver celle i kroppen fungerer som en sender og mottaker av ekstracellulære vesikler. Ettersom disse vesiklene bærer viktig biologisk informasjon, har de et stort potensial for medisinske bruksområder som diagnose og terapi.

I denne oppgaven studeres ekstracellulær vesikkelmediert kommunikasjon i hjernen for tidlig oppdagelse av Alzheimers sykdom. Alzheimers er et betydelig helseproblem på grunn av påvirkningen den har på pasienter, familier og samfunnet som helhet. Det er spesielt utfordrende fordi diagnosen ofte blir gjort på et sent stadium, noe som begrenser effektiviteten på tilgjengelige behandlinger. Tidlig diagnose gir pasientene og deres familier mer tid til å forberede seg til fremtiden og ta bedre beslutninger for fremtidige behandlinger og livsplaner.

Et teoretisk punkt-til-punkt kommunikasjonsmodell for ekstracellulær overføring mellom celler ble dermed etablert. Nevroner representerer både sender og mottaker av et kommunikasjonssystem, mens den ekstracellulære matrisen i hjernen representerer forplantningskanalen. I tillegg undersøkes effekten av Alzheimers på den definerte koblingen, forutsatt at ytelsen til kommunikationskoblingen kan tjene som en biomarkør for utviklingen av sykdommen, og hjelpe til med tidligere diagnose.

Acknowledgement

I would like to express my sincere appreciation to my supervisor, Mladen Veletić, and my co-supervisor, Martin Damrath, for their constant support and invaluable guidance from the beginning to the end of this thesis. I am deeply grateful for their time, assistance, feedback, and advice. Their unwavering support, including weekly meetings throughout these months, made a significant difference in completing this thesis.

I would like to thank Professor Ilangko Balasingham for introducing me to an exciting research field and supporting my passion for it.

From the bottom of my heart, I want to thank my family and friends for encouraging me throughout my time as a student. Their love and belief in me have been a great source of motivation and confidence.

In memory of my grandma, whose eyes shone with love, even when she couldn't remember me.
This is for her and everyone affected by Alzheimer's disease.

Table of Contents

| | |
|--|-----------|
| List of Figures | ii |
| Abbreviations | iv |
| 1 Introduction | 1 |
| 1.1 Motivation | 1 |
| 1.2 Background | 2 |
| 1.3 Hypothesis and Objective | 3 |
| 1.4 Outline | 3 |
| 2 Point-to-point Communication Model | 4 |
| 2.1 Transmitter | 6 |
| 2.2 Channel | 8 |
| 2.2.1 Diffusion-advection Equation | 9 |
| 2.2.2 PIC Model | 11 |
| 2.3 Receiver | 12 |
| 2.3.1 ODE-based Model | 12 |
| 2.3.2 PIC Model | 13 |
| 3 Results | 15 |
| 3.1 Diffusion-advection Model | 15 |
| 3.2 PIC Model | 17 |
| 4 Discussion | 20 |
| 4.1 Release | 20 |
| 4.2 Propagation | 23 |
| 4.2.1 Diffusion-advection Model | 23 |
| 4.2.2 PIC Model | 26 |
| 4.3 Uptake | 27 |
| 4.4 End-to-end Model | 29 |
| 5 Conclusion and Future Work | 30 |
| References | 31 |
| Appendix | 34 |

List of Figures

| | | |
|----|--|----|
| 1 | Transmission between neurons, created with BioRender.com. | 4 |
| 2 | Brain affected by AD, created with BioRender.com. | 5 |
| 3 | Modeling the communications between neurons as a communication system. | 5 |
| 4 | EV release, created with BioRender.com. | 6 |
| 5 | Extracellular matrix of brain, created with BioRender.com. | 8 |
| 6 | EV uptake mechanisms, created with BioRender.com. | 12 |
| 7 | End-to-end model. | 14 |
| 8 | Bound and internalized EVs from solving the system of ODEs (21), healthy case. . . | 16 |
| 9 | Bound and internalized EVs from solving the system of ODEs (21), unhealthy case. . | 17 |
| 10 | Bound and internalized EVs from the PIC model, healthy case. | 18 |
| 11 | Bound and internalized EVs from the PIC model, unhealthy case. | 19 |
| 12 | Control signal and the corresponding sequence of action potentials in the responding neuron. | 20 |
| 13 | Microdomain calcium concentration affected by the control signal. | 21 |
| 14 | EV release rate, healthy case. | 21 |
| 15 | EV release rate, unhealthy case. | 23 |
| 16 | Channel impulse response of (9). | 24 |
| 17 | Channel output with the channel impulse response from (9). | 25 |
| 18 | Probability function of EVs concentration at different r positions, healthy case. . . | 26 |
| 19 | Probability function of EVs concentration at different r positions, unhealthy case. . | 27 |
| 20 | Bound and internalized EVs from MM approach in (24). | 28 |

Abbreviations

- **AD** Alzheimer's Disease
- **CT** Computed Tomography
- **ECM** Extracellular Matrix
- **EV** Extracellular Vesicle
- **fMRI** Functional Magnetic Resonance Imaging
- **MC** Molecular Communications
- **MM** Michaelis-Menten
- **MRI** Magnetic Resonance Imaging
- **MS** Multiple Sclerosis
- **NTNU** Norwegian University of Science and Technology
- **ODE** Ordinary Differential Equation
- **PET** Positron Emission Tomography
- **PIC** Particle Intensity Channel

1 Introduction

1.1 Motivation

The number of people with dementia worldwide is estimated to increase from approximately 55 million in 2019 to 150 million cases in 2050 [1]. The most common type of dementia is Alzheimer's disease (AD), which is a progressive disease associated with loss of memory, communication with the surroundings, and cognitive function [2], [3]. Patients with AD gradually lose their ability to do daily tasks. The impact of AD is expected to further rise with the aging population and increased life expectancy.

The disease can have consequences that affect not only the patient and their family members but also the society as a whole. Witnessing a loved one's decline can lead to increased stress, anxiety, and even depression among family members. It can strain relationships and impact the overall well-being of caregivers, affecting their ability to fulfill other responsibilities and participate fully in society. The costs of medications and long-term care services can be too high for families. Moreover, the economic impact extends to healthcare systems, including hospitals and nursing homes [4].

AD is a complex condition influenced by various factors. These factors include age, genetics, head injuries, vascular diseases, infections, and environmental elements like heavy metals [2]. The exact cause of AD is still not clear, but it has been evidenced that the accumulation of amyloid beta ($A\beta$), the hyper-phosphorylation of tau, and other factors like synaptic loss, oxidative stress, and neuronal death are important elements in the development of the disease [5].

Currently, the available medicine do not target the root causes of AD and cannot cure it or stop its progression [6], [3]. The approved treatments either mitigate the symptoms of AD or slow the progression of the disease as explained on Alzheimer's Association website [7]. Based on the information provided, one approach is amyloid-targeting treatment, which aims to slow down AD progression by removing amyloid-beta plaques. Examples of anti-amyloid antibody therapies like Aducanumab (Aduhelm™) and Lecanemab (Leqembi™) have shown positive outcomes in reducing cognitive and functional decline in individuals with early-stage AD. Other medications such as donepezil, galantamine, and rivastigmine help treat cognitive symptoms like the decline in memory and thinking. These drugs work by positively affecting certain chemicals in the brain that are involved in the communication between neurons. Although these drugs cannot completely stop the damage to brain cells, they may help reduce or stabilize symptoms for a limited time.

The symptoms of AD do not immediately appear after the person develops the disease, which then leads to a late diagnosis of the disease. Symptoms such as memory loss, difficulty in communication, and confusion can gradually progress over the years and become more noticeable in the later stages [8]. The characteristic features of AD, namely $A\beta$ plaques and neurofibrillary tangles, can be observed in the brain long before individuals exhibit noticeable cognitive decline [9], [10]. This indicates that the disease may start developing well in advance of any obvious symptoms. Consequently, many people in the early stages of AD may not even realize they have the condition, as their memory and thinking abilities are still relatively intact for their daily activities [11].

Early diagnosis of AD is important for providing relevant information, resources, and support to individuals, helping them make the most of their abilities and benefit from available treatments. Although the disease still does not have a known cure, and the current medications primarily treat the symptoms of AD [2], diagnosing the disease in the earlier stages can help doctors in prescribing appropriate treatment, which can slow down the progress of the disease and enhance the quality of life of patients. It will also allow for communication about the changes they are experiencing with family and friends. Moreover, early diagnosis helps people with AD live independently longer, avoiding unnecessary care home or hospital admissions. This improves their quality of life and reduces long-term care costs [4].

In detecting the impact of AD, one aspect that can be explored is the potential influence of disease biomarkers as parameters of AD on molecular communication within the brain. It is hoped that investigating the impact of the disease on communication performance between the cells, here

neurons, has the potential to serve as a valuable tool in diagnosing and identifying AD.

1.2 Background

Currently, the diagnosis of AD cannot be made by only one tool, and the existing diagnosis method for AD is a combination of different tests [12]. The doctors check patients' medical records and consider if there is a family history of AD or similar conditions. Physical tests, such as checking blood pressure and temperature and collecting blood or urine samples, can help determine if there are other diseases like depression and thyroid problems, vitamin deficiencies, and medication side effects that have caused symptoms similar to AD's. Conducting neurological exams, assessing their cognitive and functional abilities, and using brain imaging techniques are also other tools that are used in the diagnosis of AD.

The current diagnosis tools can mainly detect AD after symptoms have started, which means that the disease has already caused severe and probably irreversible brain damage [13]. However, researchers are aiming to find biomarkers that can help diagnose AD before the symptoms appear. This includes using techniques like structural, functional, and molecular imaging. Structural imaging, like magnetic resonance imaging (MRI) and computed tomography (CT) scans, helps see the change in shape and size of the brain. Functional imaging, including positron emission tomography (PET) and functional MRI (fMRI), shows how active different parts of the brain are. Molecular imaging uses PET and fMRI to check the chemical and cellular changes that can be related to the disease. These imaging techniques help researchers learn more about AD and find ways to diagnose it earlier.

Diseases such as multiple sclerosis (MS), AD, and paralysis are highly associated with problems in cell communication [14]. Communication in biological systems often occurs through (macro)molecules, for example, vesicles in intracellular communication, neurotransmitters in intercellular communication, and hormones in interorgan communication [15], [16]. In molecular communication, information molecules trigger reactions in the recipient, resulting in the re-creation of specific phenomena or chemical states that the sender intended to transmit [17].

Molecular communications (MC) is a rapidly growing field that combines biology, information and communication theory, and engineering to explore how organisms communicate at the molecular level. This field has diverse applications, from biomedical engineering to synthetic biology to biomedical engineering [18]. One application is biochemical sensing, which involves using MC to detect and monitor specific chemicals in the body for medical diagnosis and disease tracking. MC also enables the creation of artificial cellular networks to coordinate complex biological processes. In the field of biomedical implants, MC enhances the communication between implanted devices and surrounding cells or tissues, improving their functionality.

By understanding how information molecules are transmitted, MC has the potential to aid in the diagnosis and treatment of various diseases. Different applications of MC are in the field of medicine [19]. MC can be very helpful in diagnosing diseases, for example, the early detection of tumors by monitoring specific biomarkers in the body's circulation. This approach can help identify different types of cancer at an early stage, enabling timely treatment. MC has many applications in medical treatment. It can be used for the triggering of the immune system, nanosurgery, and monitoring, control, and delivery of drugs.

Targeted delivery of drugs for disease treatment is a recognized application of MC. The applications of MC in drug delivery are valuable, as it improves how medicines are transported in the body. Unlike traditional methods, MC allows for precise and controlled delivery of drugs. As explained in [18], by using specialized carriers called drug-loaded vesicles, drugs can be enclosed and released at specific locations in the body. These carriers travel through the bloodstream and reach their intended targets. The drugs are released based on specific signals or conditions, ensuring they are delivered only where and when needed. This targeted approach reduces side effects and enhances the effectiveness of treatment, especially in cancer therapy. Ongoing research aims to enhance MC-based drug delivery systems for personalized medicine and more efficient treatments.

1.3 Hypothesis and Objective

Extracellular vesicles (EVs) play an important role in molecular communication. These tiny structures are released by cells into the extracellular space and carry various molecules, such as proteins and nucleic acids, that allow cells to communicate with one another [20]. They serve various important functions in the body, such as removing cellular waste, defending against foreign invaders, regulating gene expression, and activating the immune system [21]. EVs have the prospect of being used in the diagnosis and treatment of diseases. Examining the EV distribution has the potential to act as an indicator of changes in the acidity level of the tumor microenvironment [21]. This can provide insight into the acidification status of the tumor microenvironment, which can aid in designing targeted therapies and diagnostic strategies for cancer. Moreover, EVs can be found in various body fluids and can be used for drug delivery for treating some of the disorders [20].

EVs have gained interest in AD diagnosis due to their ability to carry biomarkers indicating chronic and degenerative diseases. Advanced proteomic techniques have revealed that EVs reflect cellular changes in both normal and pathological conditions [22]. Researchers are investigating the role of EVs in AD progression, as cellular abnormalities in endosomes, lysosomes, and mitochondria are early signs of neurodegenerative processes such as Alzheimer's and Parkinson's. Dysfunctional organelles affect EV production and release in the brain. Also, genetic risk factors for neurodegenerative diseases involve proteins associated with endosomal and lysosomal trafficking. Disruptions in the cellular system result in impaired protein degradation and altered sorting, influencing the molecular content of EVs. This knowledge can help improve the diagnosis and understanding of AD.

The objective of this thesis is, however, to theoretically describe and numerically simulate an end-to-end communication model within the brain utilizing MC methodology. The focus will be on the cell-to-cell transmission of EVs, which have a major impact on communication between healthy and diseased cells.

To achieve this, an end-to-end communication model is defined for the transmission of EVs within the brain. The model includes transmitting neurons, receiving neurons, and the propagation channel, taking into account biological phenomena in molecular communication, such as action potentials, tortuosity, receptor binding, etc. The focus is on developing a point-to-point communication theoretical model, where the communication performance can be evaluated by the number of received information particles, here the EVs. The model will gain relevant insights into EV communication in the brain environment and can serve as the basis of an advanced computational tool for pre-clinical and clinical studies.

Additionally, the study investigated the changes in communication performance when the communication link is affected by AD. To model the disease, the relevant parameters of the communication link are explored and modified accordingly.

The goal of this study is to gain a better understanding of how cell-to-cell communication is affected by AD. The research is hoped to contribute to the development of diagnostic methods that can detect the disease early and help improve the outcomes for people suffering from it.

1.4 Outline

The report is organized into the following chapters. Chapter 2 discusses the research methodology, including the system model of the EV-mediated point-to-point communication link in the brain. It provides detailed explanations of how each component, such as the transmitter, channel, and receiver, is modeled. In Chapter 3, the simulation results of the developed point-to-point communication model are presented. A comparison is made between healthy and unhealthy cases, highlighting the impact of AD on cell-to-cell communication in the brain. These results are further discussed in Chapter 4, which also presents the intermediate result for each component of the communication model. The final chapter, Chapter 5, concludes the report, summarizing the key findings and discussing potential future directions for research.

2 Point-to-point Communication Model

Neurons communicate in different forms through a combination of electrical and chemical signals [23]. Communication occurs through synapses. Also, neurons can have long-range communication through the diffusion of signaling molecules in the extracellular space.

An MC transmitter releases tiny particles like molecules or lipid vesicles into a liquid or gas medium [24]. EVs are small vesicles released by cells and they play a crucial role in intercellular communication by transferring active biomolecules to nearby and distant cells [21].

After EVs are generated by transmitting cells, they are released into the extracellular space by the formation of the multivesicular bodies and fusion with the plasma membrane [25]. The released EVs from the transmitting cells, when transported through the extracellular space, can be affected by the surroundings and environment. Transportation between cells can be subject to different propagation mechanisms such as diffusion-based or flow-based mechanisms. On the receiver side, the number of received EVs, their delay, and their concentration can be used as a metric to evaluate the communication link performance [26]. Figure 1 illustrates the point-to-point EV-mediated communication between cells, here neurons.

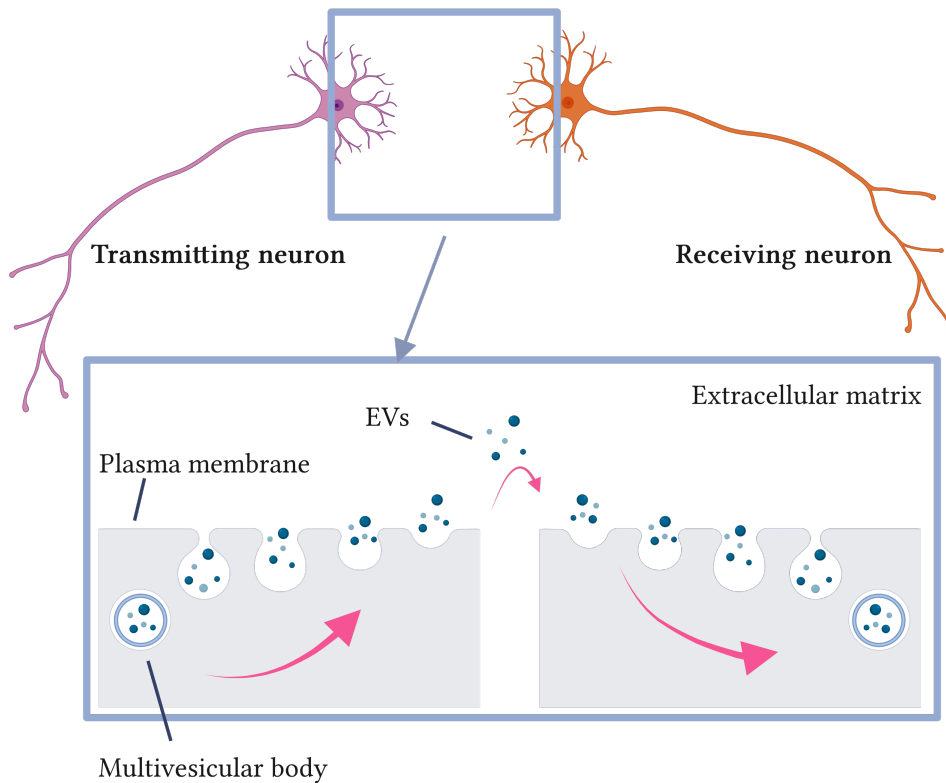


Figure 1: Transmission between neurons, created with BioRender.com.

To investigate how AD can affect cell-to-cell communication, it is important to understand how the disease is developed in the brain. The exact cause of the pathological changes observed in AD remains unknown, but there are two theories that are widely accepted [2], [27]. As shown in Figure 2, there are two types of changes that can occur in the brain affected by AD. The first type is “positive” changes, which are caused by accumulation, such as the buildup of neurofibrillary tangles, amyloid-beta plaques, and other substances in the brain. The second type is “negative” changes, which are due to loss, caused by the loss of neurons, neuropil, and synapses in the brain

and the reduction in brain volume [2].

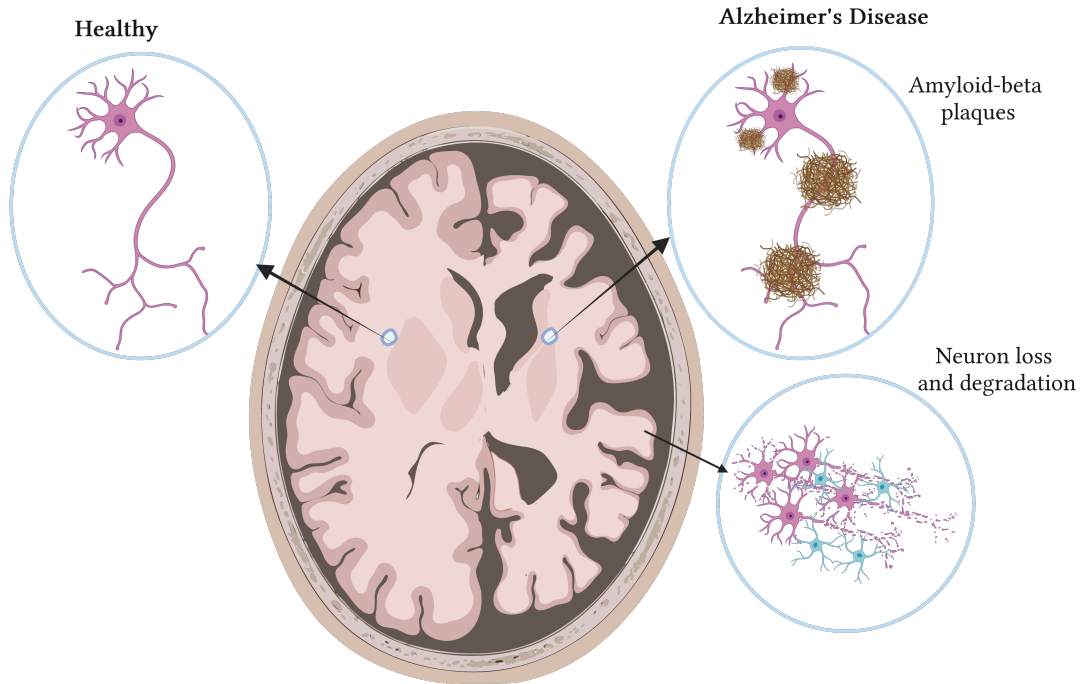


Figure 2: Brain affected by AD, created with BioRender.com.

AD is a disorder that begins to develop many years before the first signs of cognitive symptoms become apparent [28]. Understanding how the progression of the disease affects the cell-to-cell communication in brain can provide opportunities for earlier diagnosis of the disease.

All communication systems are made up of three main components: transmitter, channel, and receiver. This chapter aims to model the communication between neurons with the communication system components, as shown in Figure 3. A mathematical model for each component is defined in the following and it is explored how AD can affect each part. At the end of the chapter, transmitter, channel, and receiver models are combined together to form an end-to-end model for cell-to-cell communication in the brain.

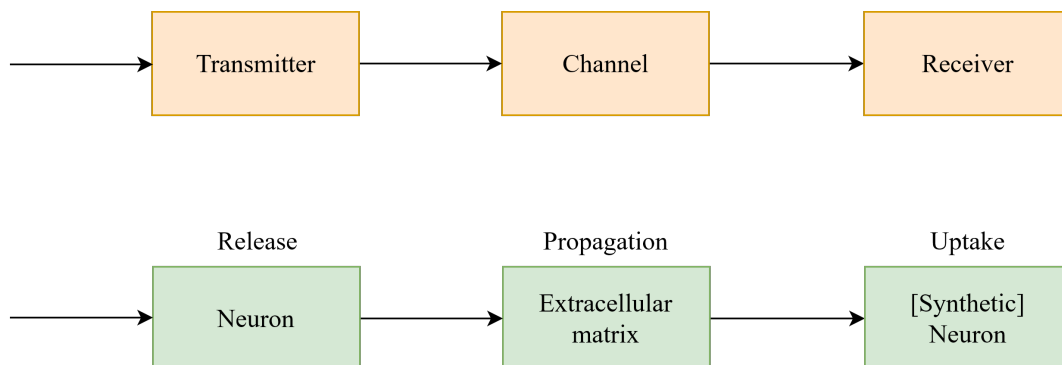


Figure 3: Modeling the communications between neurons as a communication system.

2.1 Transmitter

In the communication system, the transmitter's function is to generate and transmit a signal that carries the information. In this context, transmitting neurons will initiate cell-to-cell communication by releasing EVs that contain molecules to be transported to the receiving neurons. Cells release EVs to communicate and transfer biomolecules between themselves.

To model the transmitter in the point-to-point communication link, it is essential to understand how the EVs are released from neurons. EVs are packed in multivesicular bodies [20] and are released from inside neurons into the extracellular space through the exocytosis process as explained in [29]. The exocytosis process involves the fusion of the multivesicular bodies with the cell membrane, as shown in Figure 4. This causes the EVs to be released outside, which allows communication between neurons [30].

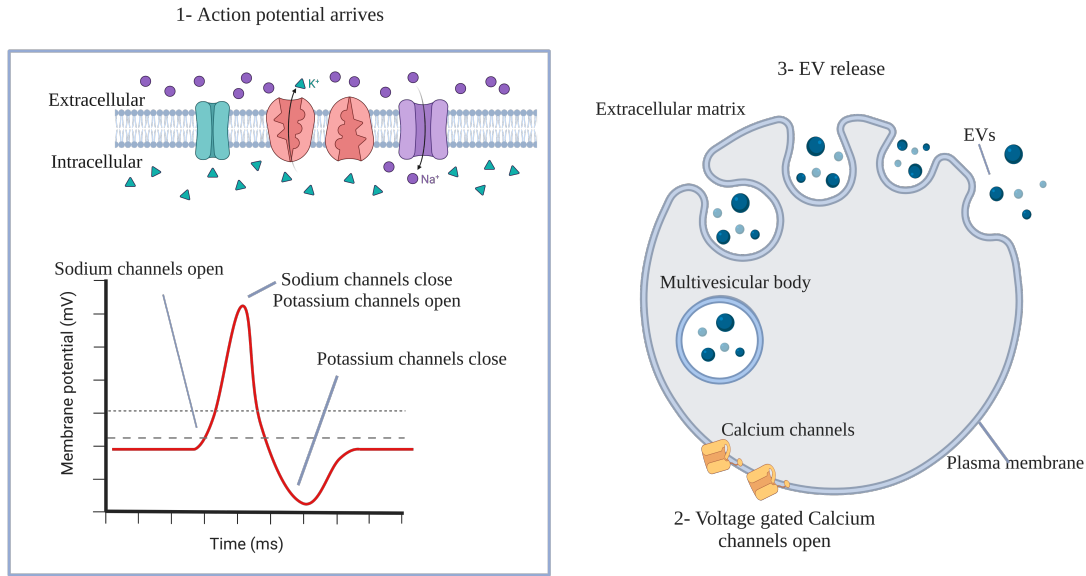


Figure 4: EV release, created with BioRender.com.

In [31], a mathematical model to simulate the release of EVs from differentiated induced neural stem cells was developed. The model was defined for the EV release from neurons and astrocytes, aiming to understand and predict the dynamics of EV release in the context of targeted drug delivery. As shown in this work, in many cells, intercellular calcium signaling controls exocytosis, leading to the release of the vesicles into the extracellular environment. Based on this, in our proposed model, the role of Ca^{2+} concentration is taken into account to observe the exocytosis activities process.

When a neuron is activated, it depolarizes and triggers electrical activity, which involves the opening of voltage-gated Ca^{2+} channels [32]. This opening allows calcium ions to flow into the neuron, causing an increase in the concentration of calcium in the cell. The rise in calcium concentration then triggers the release of various EVs.

The transmitter model is defined based on the solution from [31], which defines a link between calcium concentration and the electric activity of the cells. Here, to model the transmitter, the Hodgkin-Huxley model is used to represent the electrical activity of the neurons. The Hodgkin-Huxley model is a mathematical model that explains how the changes in membrane voltage trigger two types of currents: a fast inward current carried by Na^+ ions and a slower outward current carried by K^+ ions [33]. This model is conductance-based and is based on the concept that ion channels present in the neuron's membrane allow specific ions to pass. The opening and closing of these channels are influenced by the changes in electrical potential across the membrane. Based on the Hodgkin-Huxley model, the membrane potential can be defined as a function of the voltage-

gated potassium and sodium channels as

$$\frac{dv_m}{dt} = \frac{-1}{c_m} [g_K(v_m - V_K) + g_{Na}(v_m - V_{Na}) + g_L(v_m - V_L) - i_m], \quad (1)$$

where, v_m is the membrane potential, V_K and V_{Na} and V_L are Nernst potentials for potassium, sodium, and the other ions regarded as the leak channel, respectively. Membrane conductances are modeled as g_K , g_{Na} , g_L and c_m is the membrane capacitance. Also, i_m is the induced control current, which in this work is modeled as a square pulse, as it was previously modeled in [31], but in the physical case, it represents the signals from the other cells that activate the transmitting cell.

To connect the membrane potential to the calcium concentration, the Ca^{2+} current entering through the L-type Ca^{2+} channels, i_{CaL} , and Ca^{2+} currents entering through the T-type Ca^{2+} , i_{CaT} , are defined as

$$i_{CaL} = \frac{g_{CaL}(v_m - V_{Ca})}{N_L}, \quad (2)$$

$$i_{CaT} = g_{CaT} m_{CaT}^3 h_{CaT} (v_m - V_{Ca}), \quad (3)$$

where, g_{CaL} and g_{CaT} are the membrane conductance of the L-type and T-type Ca^{2+} channels and $m_{CaT}^3 h_{CaT}$ is the opening probability of the T-type channels. V_{Ca} is the Nernst potential for Ca^{2+} ions, N_L is the number of L-type channels. These currents were used in finding the microdomain calcium concentration in neurons defined in Table 1, in [31].

The fusion rates obtained by Watts and Sherman [34] are used as a basis for the modeling, where the release rate functions are determined based on the concentration of L-type Ca^{2+} microdomains ($[Ca]_L$) and sub-membrane Ca^{2+} concentrations ($[Ca]_m$). According to [31], EV release rate depending on L-type Ca^{2+} microdomains and sub-membrane Ca^{2+} concentrations in the neurons can be written as

$$R_{CaL}(t) = m_{CaL}^2 h_{CaL} F_H([Ca]_{L|opened}, K_L, n_L) + (1 - m_{CaL}^2 h_{CaL}) F_H([Ca]_{L|opened}, K_L, n_L), \quad (4)$$

$$R_{Ca_m}(t) = F_H([Ca]_m, K_m, n_m), \quad (5)$$

where F_H is the Hill function, $m_{CaL}^2 h_{CaL}$ is the opening probability of the L-type channels, and K_L , n_L , K_m , n_m are given in Appendix A-A in [31]. Normalized EV concentrations in the considered microdomains are assumed to be constant. Release rate of EVs is defined as,

$$R^{(neurons)}(t) = R_{CaL}(t) + R_{Ca_m}(t). \quad (6)$$

After modeling the release of EVs, the next step is to model the effects of AD. It is expected that the accumulation of amyloid-beta plaque affects all components of the communication link. To investigate its impacts on the release part of the link, we alter intrinsic neuronal excitability and reduce Na^+ currents. This is done based on the experimental findings [35] and [36]. In [35] experiments were done on a mouse model of AD. The study discusses the presence of altered intrinsic neuronal excitability and reduced Na^+ currents. These changes in neuronal excitability and Na^+ currents are significant factors that contribute to AD's progress. Accumulation of the $A\beta$ proteins, can lead to the decreased Na^+ current density. In the designed communication link, this can be modeled by decreasing the g_{Na} parameter. When the Na^+ conductance is decreased, fewer Na^+ ions enter the cell, leading to a weaker depolarizing current and a more challenging generation of action potentials. Therefore, altering the Na^+ conductance directly impacts the excitability of the neuron and can influence the release of the vesicles.

2.2 Channel

In the human body, communication occurs through the diffusion of molecules. Examples of this include calcium signaling between cells, synaptic communication in neurons, and intracellular communication among various cell organelles [37].

The extracellular matrix (ECM) of brain serves as a transmission channel for EVs. The concentration dynamics of EVs in the transmission channel are dependent on several factors that contribute to their movement and distribution within biological systems [20]. Diffusion, for instance, plays an important role as EVs disperse from regions of higher concentration to lower concentration areas through random molecular motion. The volume fraction of ECM plays a crucial role in their propagation, as it determines the percentage of the total tissue volume accessible to the EVs. In addition, tortuosity, which refers to the twisting, bending, or curving of brain structures, is an important factor in the analysis of EV diffusion.

Moreover, the degradation of EVs during propagation is an important factor to consider in their communication process. Furthermore, the advection of EVs occurs as they are carried along with the fluid flow, influenced by processes like interstitial fluid movement. Another influential factor is bulk flow, where EVs collectively move within the fluid, facilitating their transportation to various locations within the body. Collectively, these factors work together to shape the concentration patterns of EVs and determine their functional delivery in biological systems.

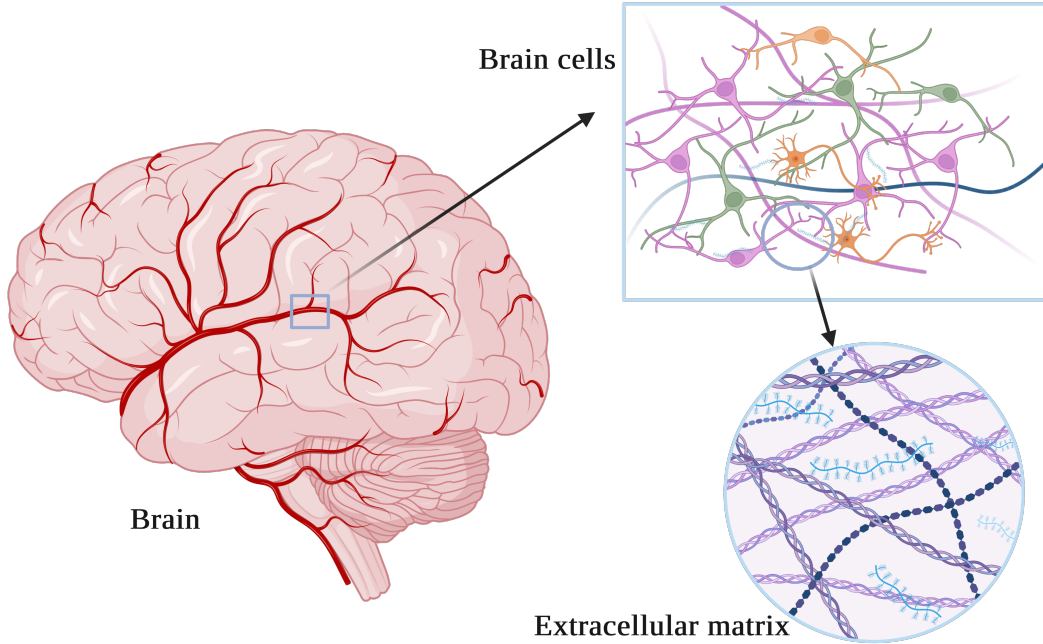


Figure 5: Extracellular matrix of brain, created with BioRender.com.

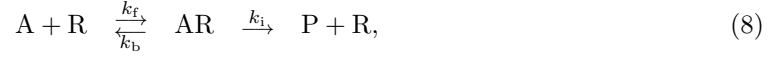
Considering ‘A’ as the unbound EVs in the channel, we assume that EVs can undergo degradation in the environment through a chemical reaction mechanism, with a degradation rate of k_d [38], and ‘ \emptyset ’ denotes that degraded EVs cannot participate in any further interactions with the receiver [39],



Here k_d can be calculated from the channel degradation parameters defined in (11).

Also, considering ‘R’ as the active EV receptor, ‘AR’ would be the EV-activated receptor formed

as a result of the reversible reaction of the receptor. Here, k_f and k_b , are forward and backward reaction rates respectively,



where ‘P’ indicates the internalized EVs and k_i is the internalization chemical reaction rate [38].

Here, we model AD’s impact on the brain ECM by increasing the tortuosity value. Based on the results of the studies done in [40], there is an observed increase in tortuosity as AD progresses. In this work, the researchers investigate a method to automatically classify subjects with AD using brain tortuosity measurements. The study explores the potential of brain tortuosity as a biomarker for the automatic classification of AD, which could aid in earlier diagnosis and treatment of the condition. This growing tendency of tortuosity is possibly associated with the erosion of brain structures and the curvature increase of cortical circumvolutions resulting from the degeneration and damage of brain tissue in AD.

In this section, the propagation of EVs is modeled using two methods, the first one is based on the diffusion-advection equation, which is solved using mathematical analysis, and a channel impulse response is derived that models the propagation of EVs in the brain ECM. The other method is based on the Fokker-Planck equation and uses the probability intensity channel (PIC) model introduced in [39]. This model considers the transport of EVs as a stochastic process and includes the receiver reactions in the channel model.

2.2.1 Diffusion-advection Equation

Aiming to model a point-to-point communication link in the brain, [20] provided valuable insight into the EVs transfer between cells. In this paper, a comprehensive end-to-end molecular communication model for EV-based drug delivery was defined. The model aimed to capture the entire process involved in EV-mediated drug delivery, from the initial release of EVs to their interaction with target cells. By considering the various stages of this communication pathway, including EV release, propagation, and uptake, the authors constructed a framework that enabled the investigation of crucial factors influencing the overall efficiency and effectiveness of drug delivery. Although the model was focused on EV transfer in heart tissues, the methods and findings of these studies have been helpful in understanding communication between brain cells.

As proposed in [20] and [31], the ECM as the EV propagation channel can be modeled based on the diffusion-advection equation.

$$\frac{\partial C(\mathbf{x}, t)}{\partial t} = \nabla(\mathbf{K}\vec{\nabla}C(\mathbf{x}, t)) - \mathbf{v} \cdot \vec{\nabla}C(\mathbf{x}, t) + \Gamma(\mathbf{x}, t, X_o) - P(t), \quad (9)$$

where $C(\mathbf{x}, t)$ denotes the EV concentration at $\mathbf{x} = (x, y, z)$ at time t . The first part of the equation models the diffusion by taking the divergence of the gradient of the EV concentration, where \mathbf{K} is the diffusivity tensor. The second part models the advection effect, where $\mathbf{v} = (v_x, v_y, v_z)$ is the velocity of ECM in three directions. The third part, $\Gamma(\mathbf{x}, t, X_o)$ is the injected EV function into the ECM, where $X_o = (x_0, y_0, z_0)$ is the release point. And the last part, $P(t)$, is modeling the degradation of EVs over extracellular binding to ECM and their half-life, which is described as

$$P(t) = \frac{1}{\sigma} \cdot \frac{C(\mathbf{x}, t)}{\alpha} + k_e \frac{C(\mathbf{x}, t)}{\alpha}, \quad (10a)$$

$$\sigma = \frac{\Lambda_{\frac{1}{2}}}{\ln(2)}, \quad (10b)$$

where the first part of (10a) shows the degradation of EVs over half-life and the second part models the degradation due to the extracellular binding. Here, $\Lambda_{\frac{1}{2}}$ is the half-life of EVs, σ is the decay

rate for the degradation of EVs with respect to the half-life, k_e is the extracellular binding rate of EVs, and α is the volume fraction of ECM, indicating the proportion of the brain occupied by the brain ECM. Based on (10), the effective degradation coefficient can be defined as,

$$k_d = \frac{1}{\alpha} \left(\frac{1}{\sigma} + k_e \right). \quad (11)$$

As in [20], (9) was defined for cardiac ECM, we simplified the equation for the brain ECM. Unlike the heart, the ECM in the brain lacks significant movement and directional flow, so we assumed the diffusivity tensor to be the same in all directions within the brain ECM. As discussed in [41], in certain regions of the brain, there can be variations in the diffusivity parameters along different axes. These variations are a result of the local anatomical structure, such as the presence of axon bundles. The diffusivity parameters become tensor quantities instead of scalar values in these cases.

Here the \mathbf{K} is assumed to be isotropic in the brain ECM due to its relatively stable and non-dynamic nature compared to highly active organs like the heart, so (12) can be simplified to,

$$\frac{\partial C(\mathbf{x}, t)}{\partial t} = K \nabla^2 C(\mathbf{x}, t) - \mathbf{v} \cdot \vec{\nabla} C(\mathbf{x}, t) + \Gamma(\mathbf{x}, t, X_o) - k_d C(\mathbf{x}, t), \quad (12)$$

here K is equal to the effective diffusion coefficient of the medium, which is calculated as $\frac{D}{\lambda^2}$, where D is the diffusion coefficient of EVs in the brain ECM and λ is the tortuosity value.

To solve the equation, the boundary conditions proposed in [20] were adopted. The selected boundary condition in this paper corresponds to a homogeneous Neumann boundary condition, assuming a constant and unaffected rate of change for the EV concentration at the boundary faces. This practical assumption is suitable for the purpose of the study, considering the natural degradation of EV concentration over time and space. By considering a static concentration at the faces of the three-dimensional (3D) space, the effects of diffusion and advection can be effectively accounted for without introducing additional complexities. Regarding the initial condition of the concentration dynamics problem, a zero concentration of EVs in the channel at the initial time is assumed.

Based on the results from [20], the solution of the diffusion-advection equation in (12), is described as the Green's function,

$$G(\mathbf{x}, t) = \frac{1}{\sqrt{4\pi K}} \exp \left[-\frac{(x - v_x t)^2 + (y - v_y t)^2 + (z - v_z t)^2}{4Kt} \right]. \quad (13)$$

Assuming the boundaries of the structure to be far from the release source [20], $C(\mathbf{x}, t)$ can be obtained from the convolution of the EV injection function with the Green's function,

$$C(\mathbf{x}, t) = \Gamma(\mathbf{x}, t, X_o) * G(\mathbf{x}, t) \quad (14)$$

and,

$$\Gamma(\mathbf{x}, t, X_o) = \frac{\gamma(t)}{\alpha}, \quad (15)$$

where $\gamma(t)$ is the EV release rate and, for simplicity of the model, is assumed to be a Dirac function in time. As we want to find the effective channel impulse response of the channel, here we chose the source function as an impulse point source. In the end-to-end model, the effective channel impulse function can be convolved with an arbitrary release function from the transmitter.

2.2.2 PIC Model

In the PIC model, the probability density function of the particle distribution can be used to model the particle transportation in the channel [39]. In this model, $p(\mathbf{r}, t|\mathbf{r}_0)$ is the probability that a given particle released at $\mathbf{r}_0 = (x_0, y_0, z_0)$, at time t_0 is at the position \mathbf{r} . Based on the assumption in [42], this probability is only dependent on the magnitude of the position vectors \mathbf{r} and \mathbf{r}_0 , denoted by r and r_0 respectively. So considering the degradation effect of the ECM, the Fokker-Planck equation representing how the probability density function of particle positions changes over time [39] can be written as,

$$\frac{\partial p(r, t|r_0)}{\partial t} = K\nabla^2 p(r, t|r_0) - k_d p(r, t|r_0). \quad (16)$$

The solution to (16) is calculated in [39] and is found to be the Green's function described as,

$$p(r, t|r_0) = e^{-k_d t} \left\{ \frac{1}{8\pi r r_0 \sqrt{\pi K t}} \left[e^{-\frac{(r-r_0)^2}{4Kt}} + e^{-\frac{(r+r_0-2a)^2}{4Kt}} \right] - \frac{1}{4\pi r r_0 \sqrt{\pi K t}} \times \left[\eta_1 W\left(\frac{r+r_0-2a}{\sqrt{4Kt}}, x_1 \sqrt{t}\right) + \eta_2 W\left(\frac{r+r_0-2a}{\sqrt{4Kt}}, x_2 \sqrt{t}\right) + \eta_3 W\left(\frac{r+r_0-2a}{\sqrt{4Kt}}, x_3 \sqrt{t}\right) \right] \right\}. \quad (17)$$

where a is the receiver radius and $W(n, m)$ is defined as

$$W(n, m) = e^{(2nm+m^2)} \operatorname{erfc}(n+m), \quad (18)$$

considering erfc as the complementary error function. The coefficient x_1 , x_2 , and x_3 can be calculated from the solution of the system of equations

$$\begin{aligned} x_1 + x_2 + x_3 &= \left(1 + \frac{k_f N_{\text{ref}}}{4\pi K a}\right) \frac{\sqrt{K}}{a} \\ x_1 x_3 + x_2 x_3 + x_1 x_2 &= k_b + k_i + k_d \\ x_1 x_2 x_3 &= \left[k_b + k_i + \frac{k_f N_{\text{ref}} k_i}{4\pi K a} - k_d \left(1 + \frac{k_f N_{\text{ref}}}{4\pi K a}\right)\right] \frac{\sqrt{K}}{a}, \end{aligned} \quad (19)$$

where a is the radius of the receiver, N_{ref} is the reference number of particles.

The constants η_1 , η_2 , and η_3 can be calculated from,

$$\begin{aligned} \eta_1 &= \frac{x_1(x_3 + x_1)(x_1 + x_2)}{(x_3 - x_1)(x_1 - x_2)} \\ \eta_2 &= \frac{x_2(x_3 + x_2)(x_1 + x_2)}{(x_2 - x_3)(x_1 - x_2)} \\ \eta_3 &= \frac{x_3(x_3 + x_2)(x_1 + x_3)}{(x_2 - x_3)(x_3 - x_1)}. \end{aligned} \quad (20)$$

The PIC model here takes the influence of the EV-receiver interaction on the EVs in the ECM into account, which is not done in (13). This model does not take into account the advection effect of the ECM but simplifies the calculation by using the spherical coordinates. If the drift can be considered in (16), the method has the potential to give good estimates of the transportation of EVs from the transmitter to the receiver.

2.3 Receiver

The released EVs from the transmitter, after being diffused in the channel are taken up by receiving cells, through different uptake processes. As shown in Figure 6, these processes include endocytosis, EV fusion with the plasma membrane, and direct interaction with the receiver cells [43]. Currently, endocytosis is recognized as the primary mechanism through which cells uptake EVs [44]. Endocytosis involves the internalization and binding of a fully intact EV by the plasma membrane, leading to its incorporation into the endosomal system [45].

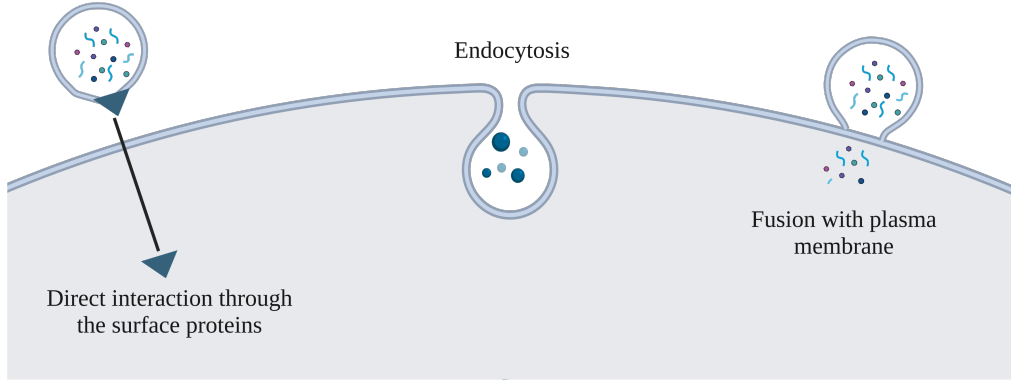


Figure 6: EV uptake mechanisms, created with BioRender.com.

Here, considering the two possible reactions in (7) and (8) for EVs released to the channel, two possible methods are developed for modeling the receiver of the point-to-point communication link. In the first approach, as a solution to the channel model in Section 2.2.1, an ODE-based model is defined for the uptake mechanisms, which needs to be solved to estimate of the number of bound EVs. The second approach uses the probability defined in Section 2.2.2 to find the detection probability at the receiver.

After reviewing relevant literature, no specific evidence was found regarding the direct impact of AD on the uptake process of receiving cells. However, the alterations in the transmitter and channel components can significantly influence the overall performance of the communication link. These modifications are important to model the impact of AD on the end-to-end link.

2.3.1 ODE-based Model

To gain insights into the cellular uptake of EVs, relevant studies from [38] and [46] were utilized. These studies provided valuable information and a deeper understanding of the mechanisms involved in the reception of EVs by recipient cells. To model the receiver, an ODE-based system model is proposed to describe various uptake mechanisms based on [38] and [20]. This system of ODEs involves a series of equations that describe the system's behavior over time based on (7) and (8).

The proposed model in [38], was modified by removing the degradation effect, as in our model this is already considered in the channel impulse response. Also, for the EVs in the environment, we assumed it to be equal to the EV concentration in the channel from Section 2.2.1.

$$\frac{dq_{\text{AR}}(t)}{dt} = k_f \cdot N \cdot q_{\text{A}}(t) - k_f \cdot q_{\text{AR}}(t) \cdot q_{\text{A}}(t) - k_b q_{\text{AR}}(t) - k_i q_{\text{AR}}(t) \quad (21)$$

$$\frac{dq_{\text{A}}(t)}{dt} = -k_f \cdot N \cdot q_{\text{A}}(t) + k_f \cdot q_{\text{AR}}(t) \cdot q_{\text{A}}(t) + k_b q_{\text{AR}}(t) + C(\mathbf{x}, t) \quad (22)$$

$$\frac{dq_{\text{P}}(t)}{dt} = k_i \cdot q_{\text{AR}}(t) \quad (23)$$

Equations (21), (22), and (23) illustrate the dynamics of bound, environmental EVs, and internalized EVs, where q_{A} is the number of EVs in the environment here the channel, q_{AR} is the number of bound EVs to the cells, q_{P} is the number of internalized EVs, and N is the total number of receptor sites per cell. During the uptake process, not all EVs will be bound to the receiving cell due to factors such as degradation and recycling, which have been modeled with a negative contribution of the corresponding coefficients. This ODE-based model does not take into account factors like how particles move or are carried by fluid, that is the advection and diffusion [38].

Analyzing the number of bound EVs can indicate the receiver's performance in the communication link. To estimate this, the coupled system can be solved with the assumption that the initial value for the bound EVs is zero. In [38], computational approaches were proposed to solve the ODE-based model of uptake mechanisms. As a result, the number of EVs in the environment, the number of bound EVs to the cell, and the number of internalized EVs could be estimated.

Michaelis-Menten (MM) approach is one of the suggested methods in [38], that can be employed when N is small compared to the number of channel EVs. MM is a simplification assumption that leads to an analytical solution and avoids numerical evaluation of the ODEs. In the MM model, it is assumed that the concentration of bound EVs is constant during the internalization period. This simplifies (21) to

$$0 = k_f \cdot N \cdot q_{\text{A}}(t) - k_f \cdot q_{\text{AR}}(t) \cdot q_{\text{A}}(t) - k_b q_{\text{AR}}(t) - k_i q_{\text{AR}}(t) \quad (24)$$

which results in,

$$q_{\text{AR}}(t) = \frac{k_f \cdot N \cdot q_{\text{A}}(t)}{k_f \cdot q_{\text{A}}(t) + k_b - k_i}. \quad (25)$$

2.3.2 PIC Model

The probabilities that released EVs are transported completely through the channel are affected by parameters such as degradation and diffusion. Using the probability of particle position defined in (17), EVs' binding and internalizing probabilities can be calculated as described in this section.

The PIC model developed in [39] defines $P_f(\tau|r_0)$ as the probability that a particle released at r_0 , and at time $t_0 = 0$ is bound to the receptor cell at τ . This can be calculated based on $p(r, t|r_0)$ from (16), defined as,

$$P_f(\tau|r_0) = \int 4\pi a^2 K \frac{\partial p(r, t|r_0)}{\partial r} \Big|_{r=a} dt. \quad (26)$$

Using the closed-form analytical expression of $p(r, t|r_0)$, the probability of bound EVs can be defined as,

$$P_f(\tau|r_0) = \frac{k_b N_{\text{ref}} e^{-k_d \tau}}{4\pi r_0 a \sqrt{K}} \left\{ \frac{x_1 W\left(\frac{r_0-a}{2\sqrt{Kt}}, x_1 \sqrt{\tau}\right)}{(x_3-x_1)(x_1-x_2)} + \frac{x_2 W\left(\frac{r_0-a}{2\sqrt{Kt}}, x_2 \sqrt{\tau}\right)}{(x_2-x_3)(x_1-x_2)} + \frac{x_3 W\left(\frac{r_0-a}{2\sqrt{Kt}}, x_3 \sqrt{\tau}\right)}{(x_2-x_3)(x_3-x_1)} \right\}. \quad (27)$$

Following this, the probability that a given particle is internalized into the receiving cell can be defined as,

$$P_i(\tau|r_0) = k_i \int_0^\tau P_f(\tau'|r_0) d\tau', \quad (28)$$

here, $P_i(\tau|r_0)$ is the detection probability or the channel impulse response of the PIC system.

This channel impulse response when convolved with the released EV from Section 2.1, can give us an estimate of the detected EVs at the receiver.

End-to-end model

Figure 7 provides a view of the entire end-to-end model. This shows how the defined methods for the transmitter, channel, and receiver can be combined to achieve the end-to-end model, in both the diffusion-advection model and PIC model.

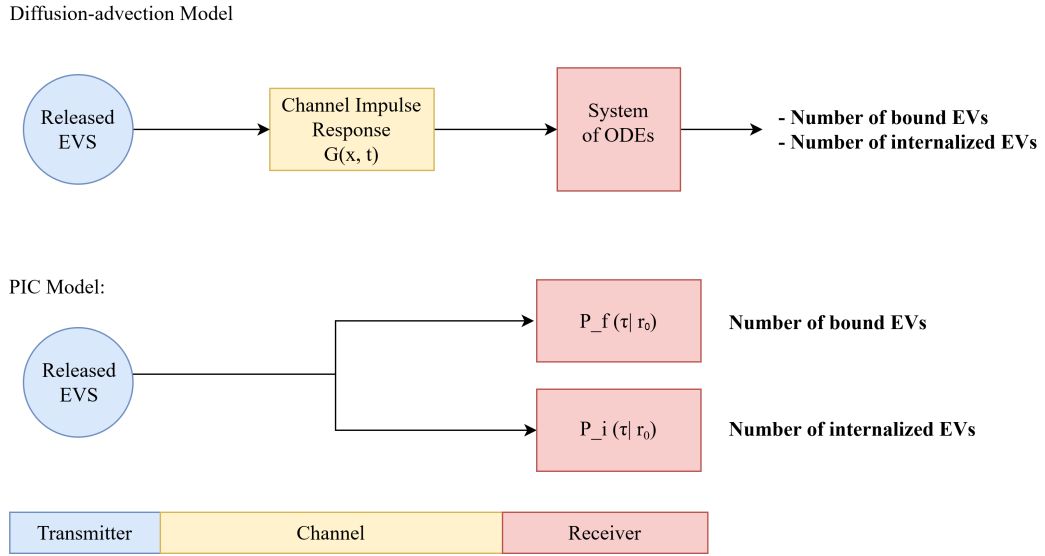


Figure 7: End-to-end model.

In Chapter 3, the results of the end-to-end models are presented. The results together with the simulation result of each component are discussed in more detail in Chapter 4.

3 Results

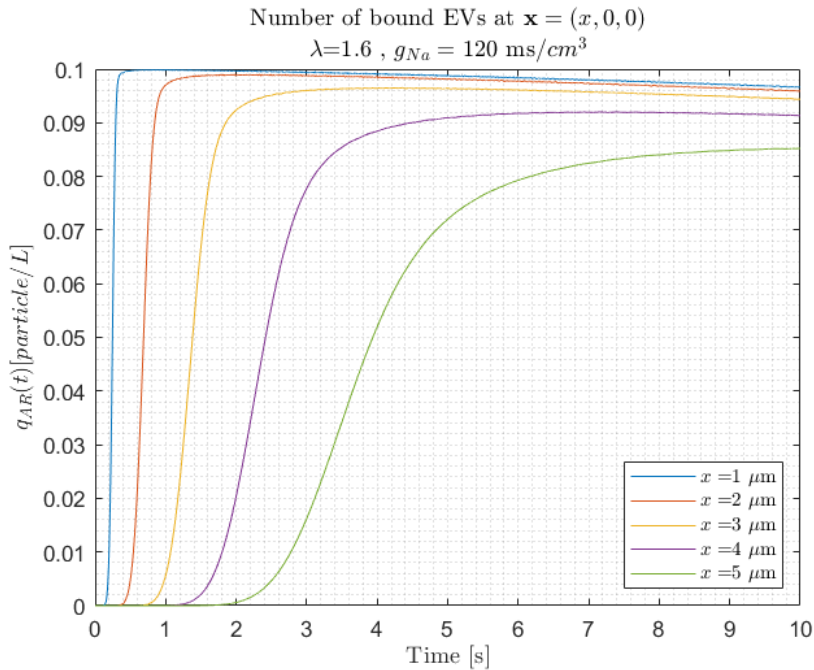
In this section, the final results from the simulation of the point-to-point communication link defined in Chapter 2 are presented. These results were obtained by combining the simulation of released EVs based on Section 2.1, propagating through the channel models introduced in Section 2.2 and being received through the uptake process modeled in Section 2.3. Moreover, the results of the healthy case are compared with those of the unhealthy case, where the communication link is affected by AD.

As discussed in Sections 2.2 and 2.3, two methods were defined to describe the end-to-end communication between neurons in the brain. The methods are the same in modeling the EVs released from the transmitting neuron but differ in how they are modeling the propagation and uptake of EVs in the channel and receiver.

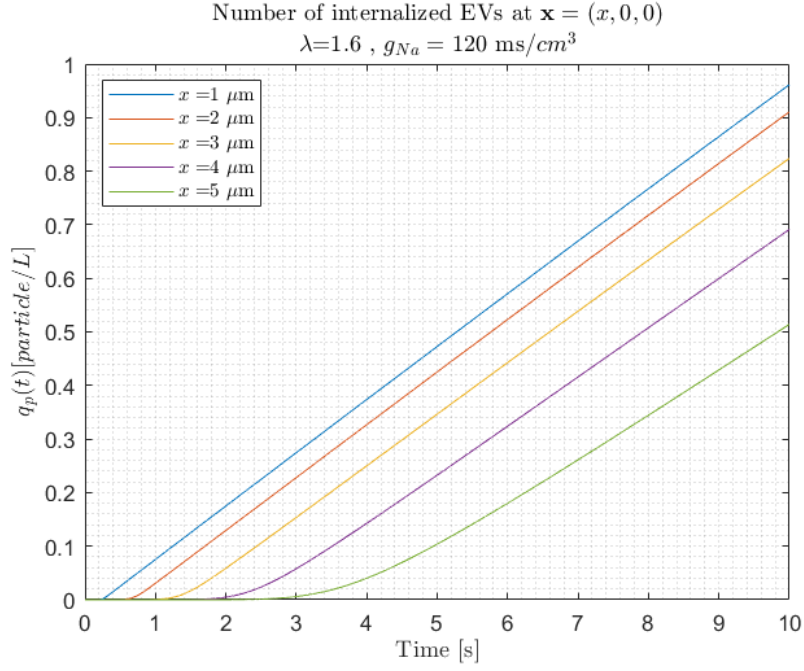
The numerical results presented in this section have been generated using the parameter values specified in Table 1. The simulation framework is implemented using MATLAB. These results are discussed in more detail in Chapter 4.

3.1 Diffusion-advection Model

As shown in Section 2.3.1, the uptake mechanisms in the receiver can be modeled as an ODE-based system model (21). This serves as the receiver model for the channel output from Section 2.2.1. Solving the system of ODEs will give the number of bound EVs, internalized EVs, and EVs in the environment, here the channel, as output. We consider the channel output from Section 4.2.1 as the number of EVs in the channel. This assumption simplifies solving ODE using the ODE solver in MATLAB. Figure 8 illustrates the number of bound and internalized EVs, assuming a zero initial condition for the system of ODE.



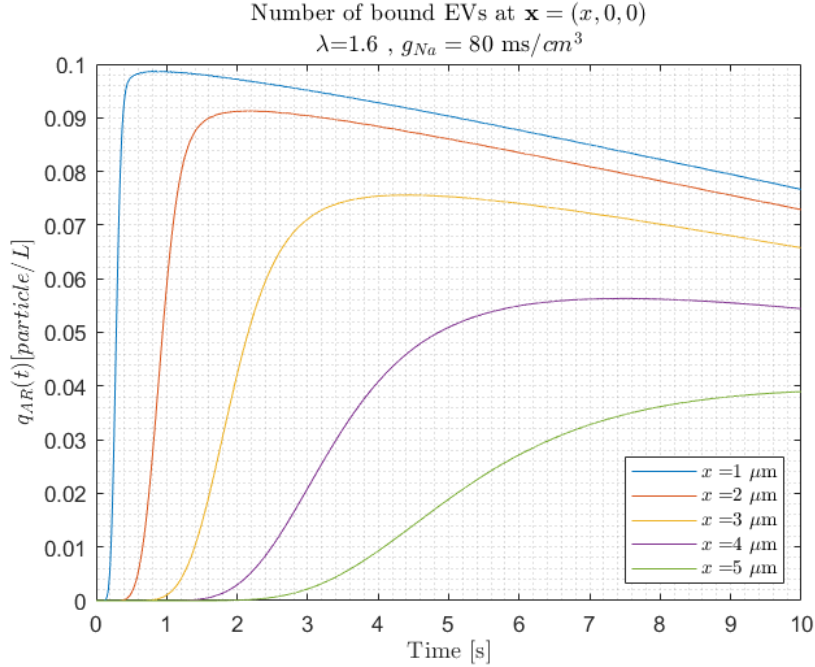
(a) Number of bound EVs.



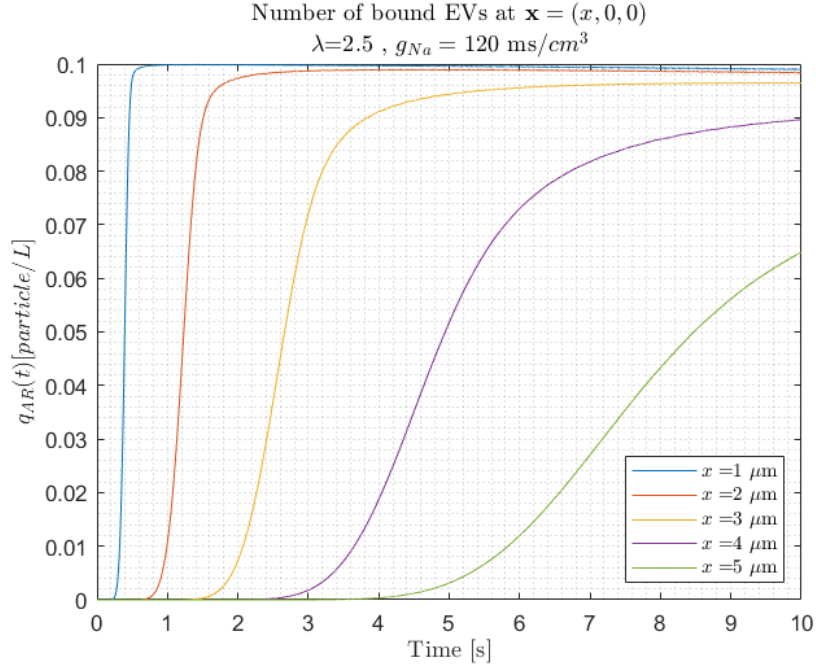
(b) Number of internalized EVs.

Figure 8: Bound and internalized EVs from solving the system of ODEs (21), healthy case.

To model AD in the communication link, modifications were made in the values of two parameters, as described in Sections 2.1 and 2.2. Figure 9a shows the number of internalized EVs in the receiver where the g_{Na} parameter is changed due to AD affecting the transmitting cell. Figure 9b, illustrates the changes in the number of internalized EVs, due to the tortuosity (λ) increase in the propagation channel, resulting from the disease.



(a) Number of bound EVs, AD affecting the transmitting cell.

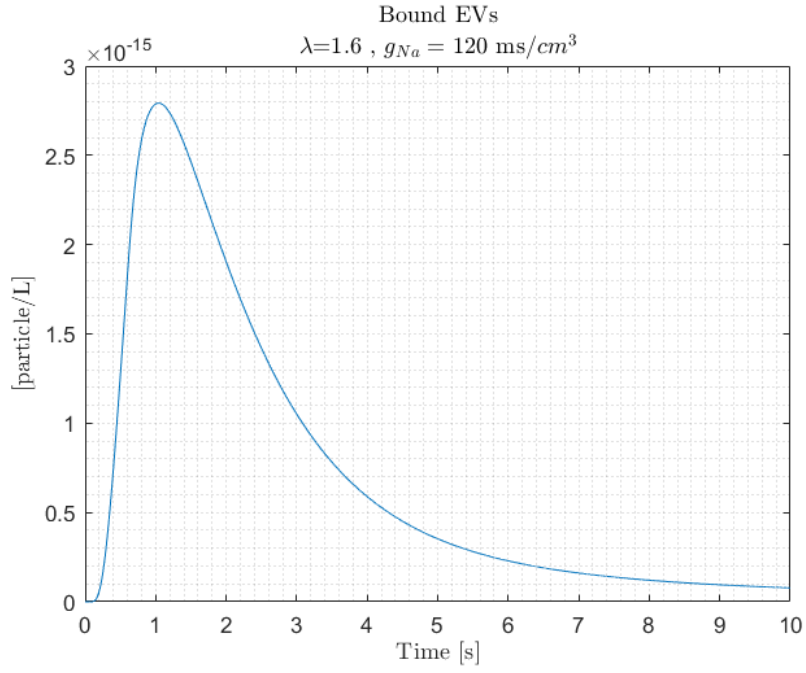


(b) Number of bound EVs, AD affecting the channel.

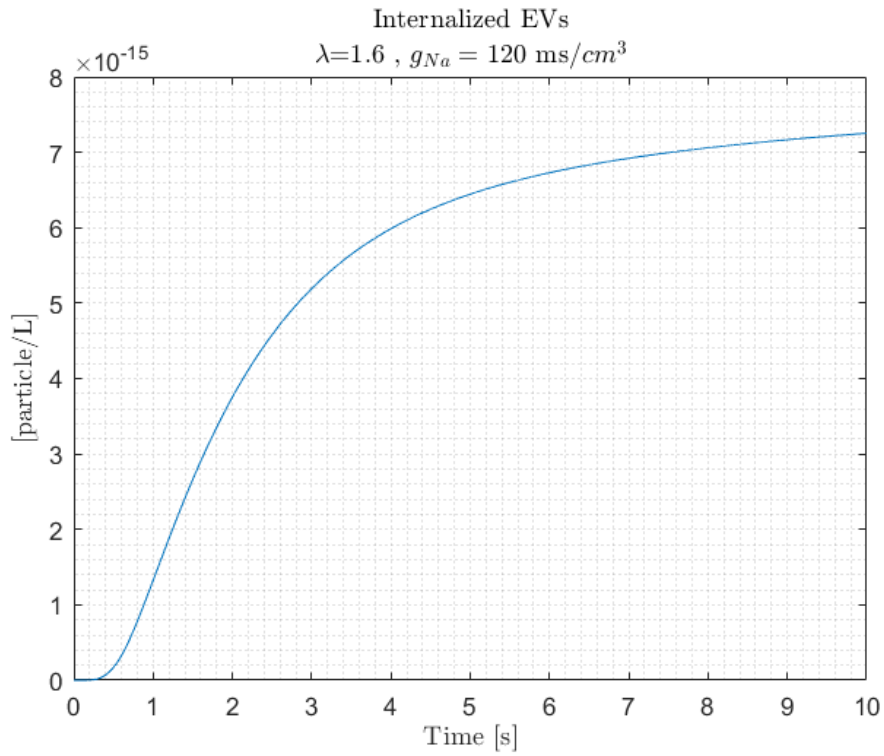
Figure 9: Bound and internalized EVs from solving the system of ODEs (21), unhealthy case.

3.2 PIC Model

In the PIC mode, the bound EVs and internalized (detected) EVs are calculated based on the channel probabilities introduced in Section 2.3.2. In this model $P_i(\tau|r_0)$ is taking into account the propagation channel effects and is modeling both the channel and the receiver binding effect. Time convolution of this probability with the released concentration from Section 2.1, results in the concentration of bound EVs, as shown in Figure 10a. The detected EVs in this model take into account the internalization process in the receiver. In the PIC model, the probability $P_i(\tau|r_0)$ is considered the channel impulse response. When the released EVs are convolved with this probability it results in the concentration of the detected EVs as shown in Figure 10b.



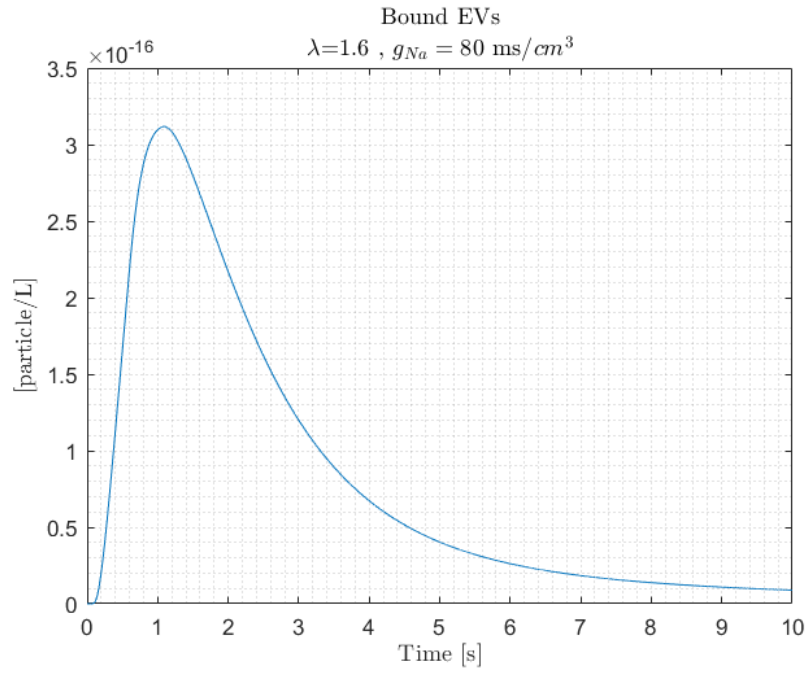
(a) Concentration of bound EVs from the PIC model.



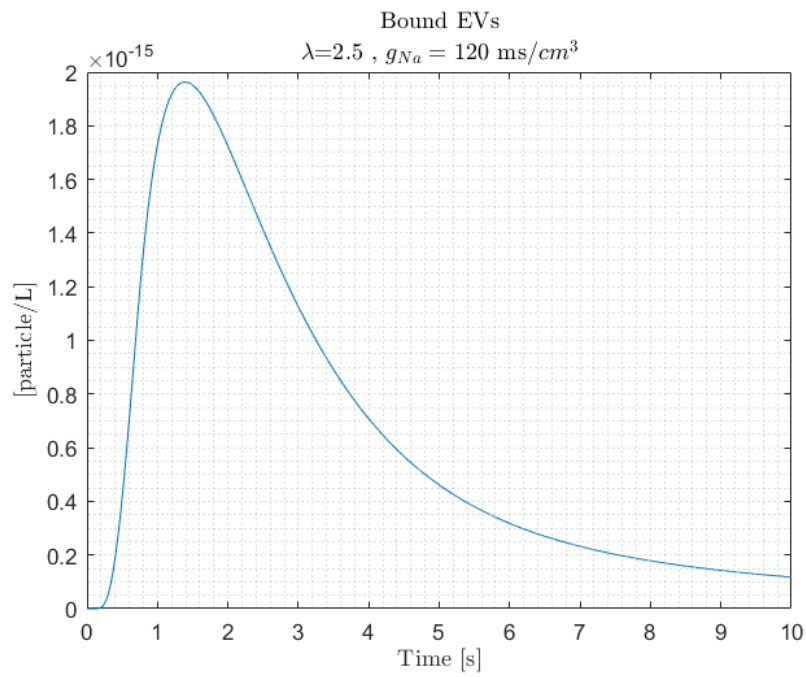
(b) Concentration of internalized EVs from the PIC model.

Figure 10: Bound and internalized EVs from the PIC model, healthy case.

Impacts of AD on the communication link of the PIC model were modeled with adjustments made to g_{Na} and λ parameters, as explained in Sections 2.1 and 2.2. Figure 11a displays how the results from PIC mode are affected due to AD's impact on the transmitter. Similarly, Figure 11b presents the changes due to an increase in the tortuosity of the propagation channel caused by the disease.



(a) Number of bound EVs, AD affecting the transmitting cell.



(b) Number of bound EVs, AD affecting the channel.

Figure 11: Bound and internalized EVs from the PIC model, unhealthy case.

4 Discussion

In this chapter, we discuss the results obtained in Chapter 3 in more detail. We examine the findings for each part of the cell-to-cell communication, which are the transmitter, channel and receiver in the communication system, and present the intermediate results we obtained along the way.

Also, we explore how AD affects the modeled communication link. The disease impacts on the EVs release rate, the concentration of EVs in the propagation channel, and the taken EVs at the receiving cell are used as the metrics to evaluate the performance of the communication link and have the potential to be utilized in the diagnosis of the disease.

The numerical results presented in this section were generated using specific parameter values listed in Table 1. To conduct our simulations, we utilized the MATLAB software framework.

4.1 Release

In Section 2.1, we discussed how the concentration of calcium plays a role in regulating the release of EVs in neurons. When neurons depolarize in response to external stimuli, the control current i_m in the Hodgkin-Huxley model (1), voltage-gated Ca^{+2} channels open and as a result, the calcium concentration changes. In the simulation, we modeled the control signal as a current pulse with an amplitude of $40 \mu\text{A}/\text{cm}^2$ and a duration of 500 ms [31]. As shown in Figure 12, a sequence of action potentials is generated in response to the stimuli. The frequency of action potentials is directly proportional to the amplitude of the external stimuli [31].

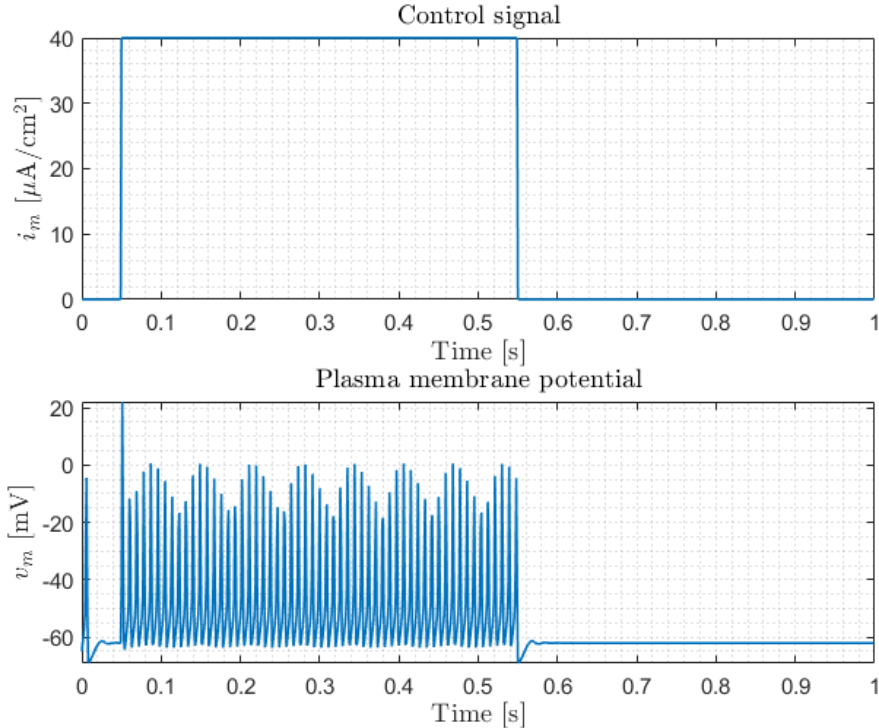


Figure 12: Control signal and the corresponding sequence of action potentials in the responding neuron.

An ODE-based system was solved in MATLAB, to calculate the changes in calcium concentration from the changes in membrane potential, based on the governing equations of microdomain calcium concentration presented in [31]. The generated action potentials control the opening of voltage-

gated Ca^{+2} , and impacting the L-type and sub-membrane calcium concentrations as shown in Figure 13.

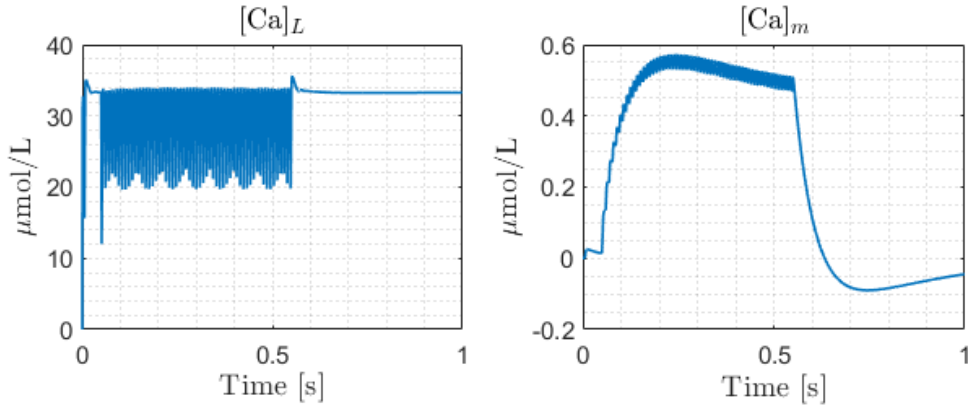


Figure 13: Microdomain calcium concentration affected by the control signal.

Based on the calculated calcium concentration, the rate of EV release can be determined using (6). Figure 14 illustrates the results of EV release in healthy neurons.

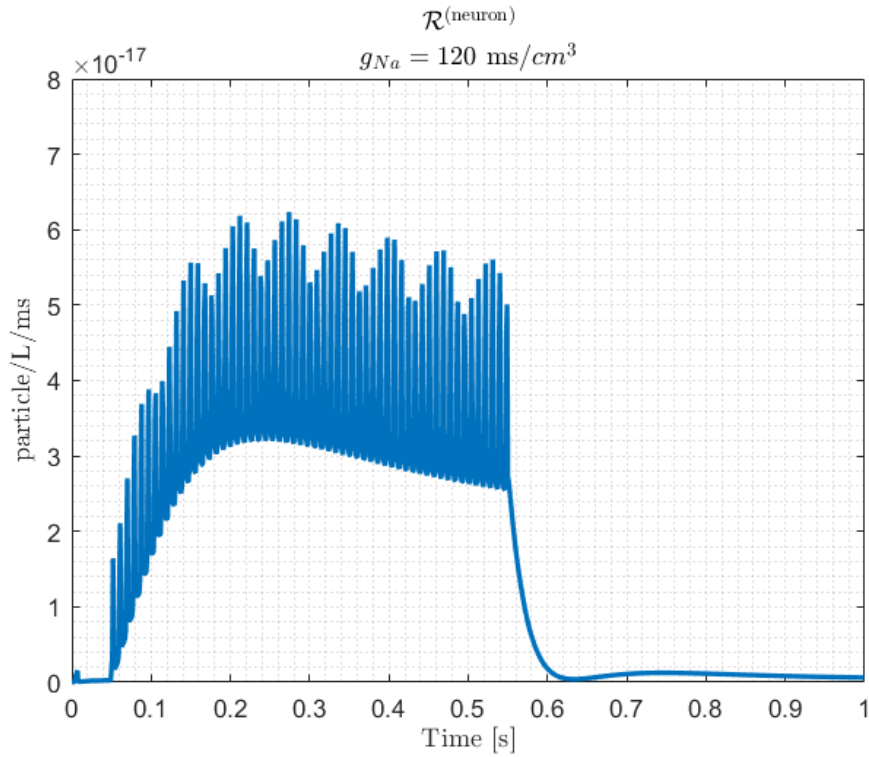
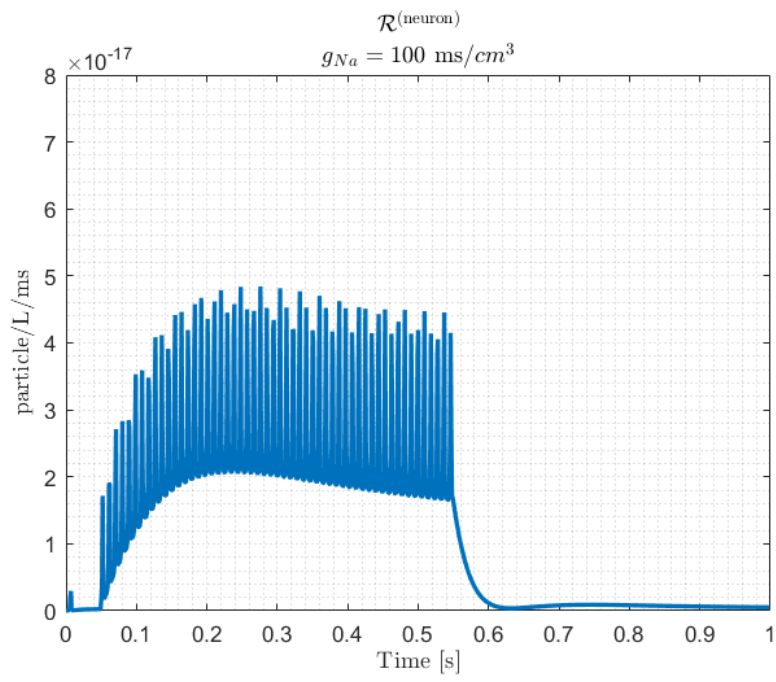
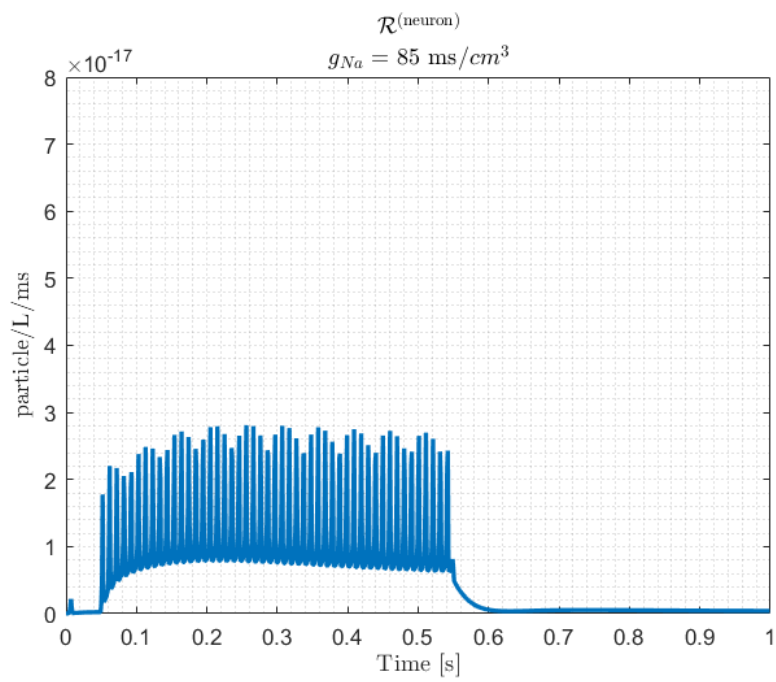


Figure 14: EV release rate, healthy case.

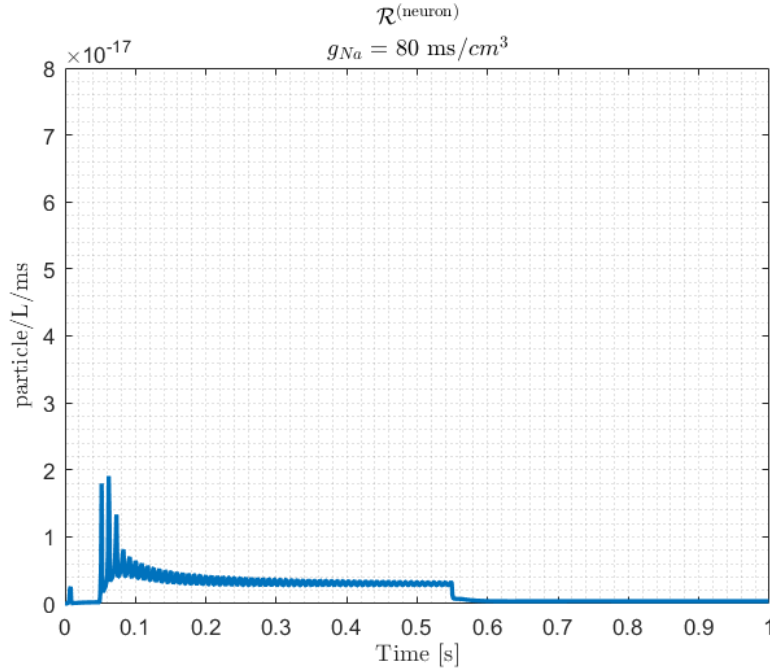
To explore how AD affects the EV release, the results were obtained while changing g_{Na} parameter gradually based on studies done in [35]. As it can be observed in Figure 15, the gradual decrease in g_{Na} , significantly reduces the EV release rate. The lowest value tested, Figure 15c, results in an altered action potential pattern where it no longer resembles a sequence of spikes.



(a) $g_{Na} = 100 \text{ ms/cm}^3$



(b) $g_{Na} = 85 \text{ ms/cm}^3$



(c) $g_{Na} = 80 \text{ ms/cm}^3$

Figure 15: EV release rate, unhealthy case.

As it can be observed, the alteration of the g_{Na} parameter in our communication link model has resulted in a lower release rate. This parameter, validated as a relevant factor for modeling AD, represents the conductance of Na^+ channels. When the conductance of Na^+ is reduced, there is a decrease in the flow of Na^+ ions into the cell. This reduction in Na^+ ions results in a weaker depolarizing current, which is necessary for generating action potentials. These results show that AD can impact the excitability of neurons and EV release, which can eventually affect the performance of cell-to-cell communication.

4.2 Propagation

In this work, the channel was simulated based on diffusion-advection (9) and Fokker-Planck (16) equations. Both models take into account volume fraction and the degradation effects of the channel. However, the diffusion-advection also models the advection effect by considering ECM velocity vector \mathbf{v} . The current PIC model based on the Fokker-Planck does not take into account the drift. On the other hand, it provides a less complex equation for calculating the output of the channel.

4.2.1 Diffusion-advection Model

In the simulation of the propagation channel based on the diffusion-advection model, the channel impulse response given by (13) was used. To calculate the output of the channel, the injection function, here the release concentrations from Section 4.1, is to be convolved with the channel impulse response. This would result in a 4D convolution. To simplify the calculation, the velocity components of ECM, v_x , v_y , and v_z were assumed to be zero, considering the lower advection effect on EVs in brain ECM compared to heart. Furthermore, the results were observed and analyzed at a specific point in space, denoted as $(x, 0, 0)$, to simplify the simulation and facilitate the plotting of the results. Figure 16 illustrates the channel impulse response for different x positions.

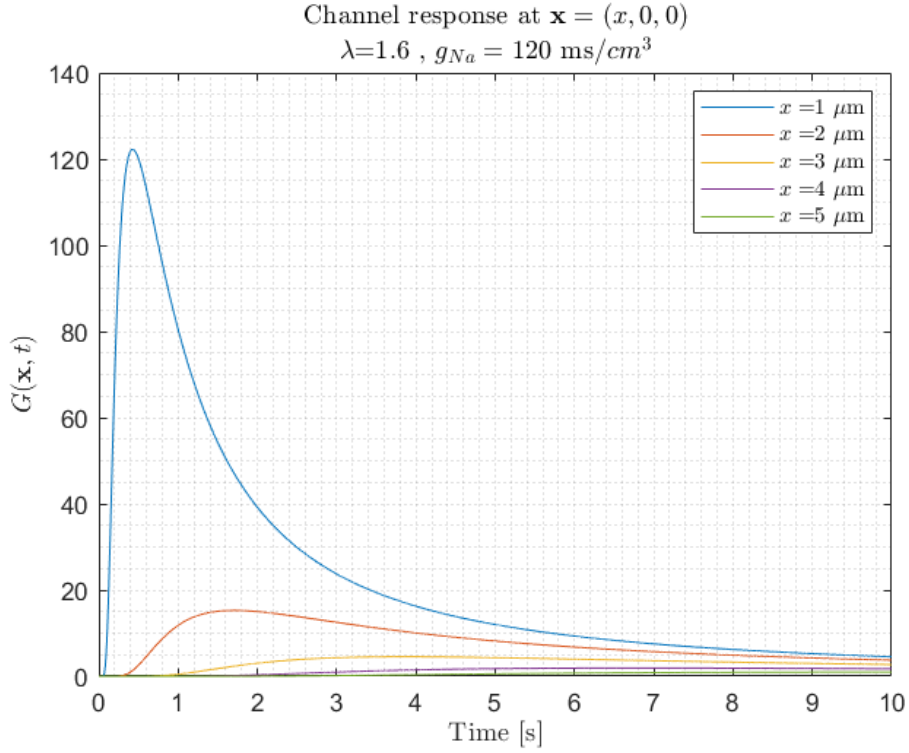
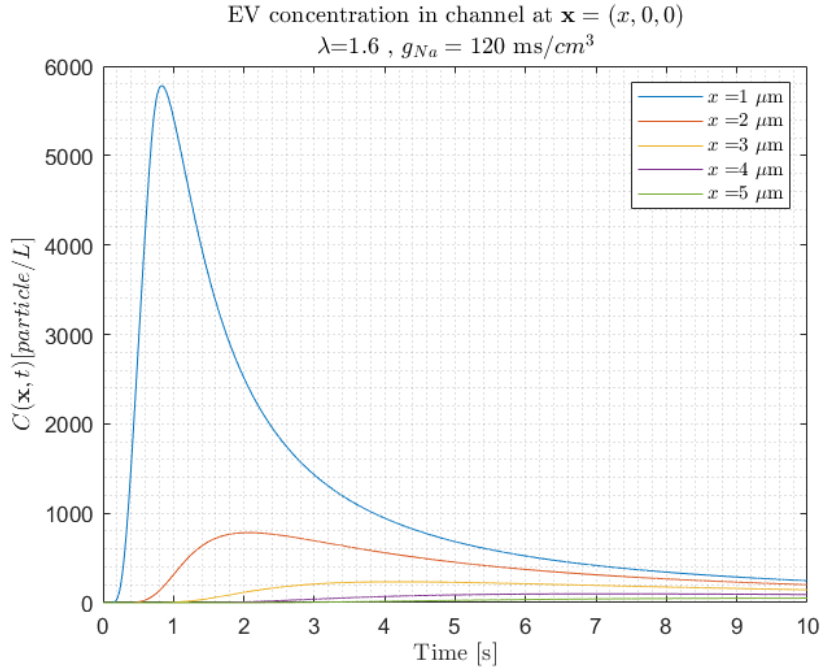


Figure 16: Channel impulse response of (9).

With simplified channel impulse response, for each x position, channel output is calculated from a time convolution between the concentration of released EVs and (13), as shown in Figure 17a. Based on the discussion in Section 2.2, in order to model AD in the propagation channel the tortuosity value, here modeled with the λ parameter, should increase. Figure 17 illustrates the concentration dynamics of EVs, with a gradual increase in λ for each x value in space.



(a) $\lambda = 1.6$

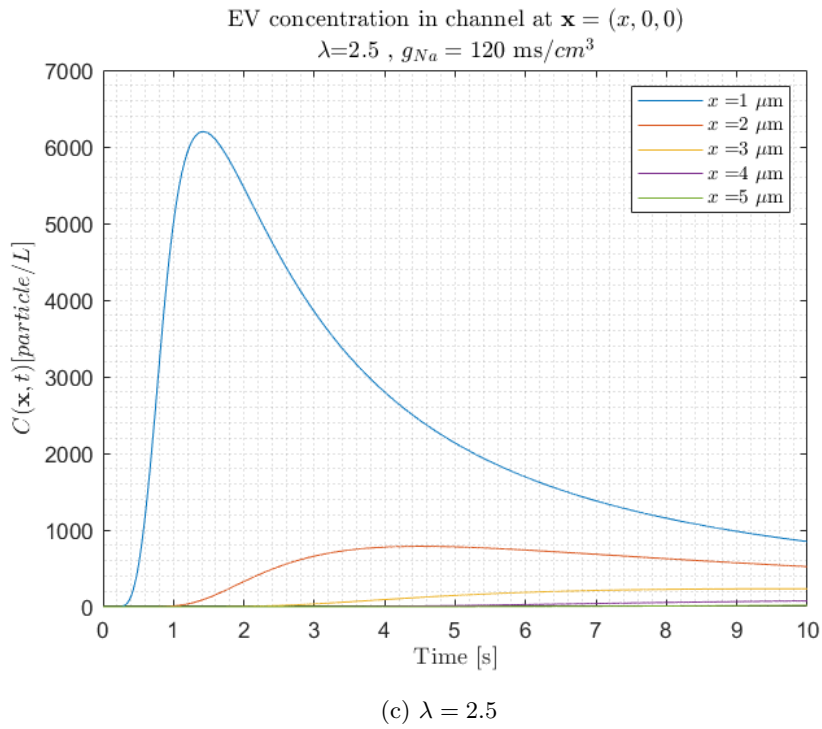
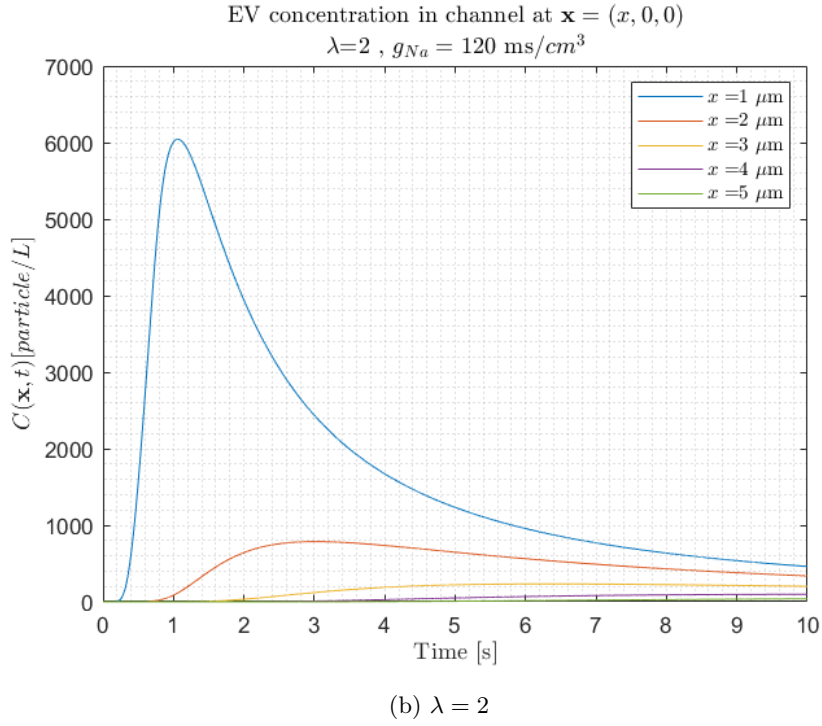


Figure 17: Channel output with the channel impulse response from (9).

As shown in Figure 17b and 17c, the increase in tortuosity affects the output of the channel, by delaying the peak of concentration for each x position. Moreover, wider concentration peaks indicate a broader distribution of concentrations over time and slower movements of EVs. This suggests that, when the ECM is affected by AD, for each x position in space, it takes more time for EVs to reach their peak concentration and longer to return to baseline levels. This can show that AD affects the propagation of EVs by slowing down or delaying the EV concentration dynamics.

4.2.2 PIC Model

The PIC model explained in Section 2.2.2, uses the Fokker-Planck equation (16) to account for the impact of the ECM on EVs. The probability function $p(r, t|r_0)$ describes how likely EVs are to be found at a particular position around the transmitting neuron. Figure 18 shows the changes in this probability over time, indicating a peak that represents the highest concentration of EVs at different r positions.

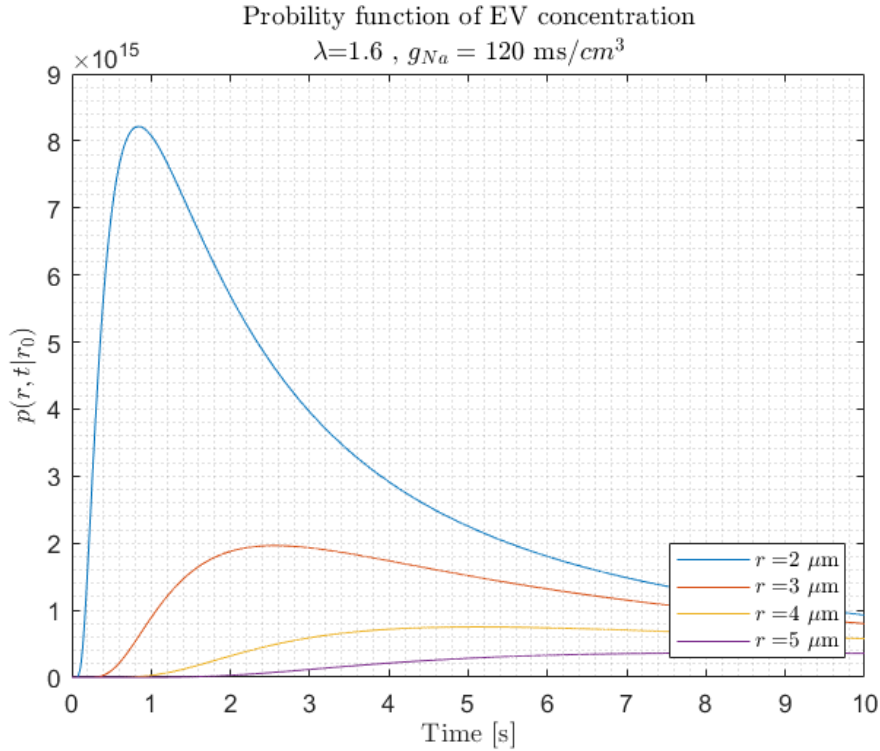


Figure 18: Probability function of EVs concentration at different r positions, healthy case.

Similar to Section 4.2.1, the AD's impact is investigated here with changing tortuosity value, as is shown in Figure 19. As can be observed, increasing the tortuosity value leads to a delay in the peak of the probability of concentration. Similar to the result from the diffusion-advection model, this indicates that as the tortuosity in the brain ECM increases due to AD, the EVs propagate slower and this leads to a flatter diagram for the probability function of concentration in the PIC model.

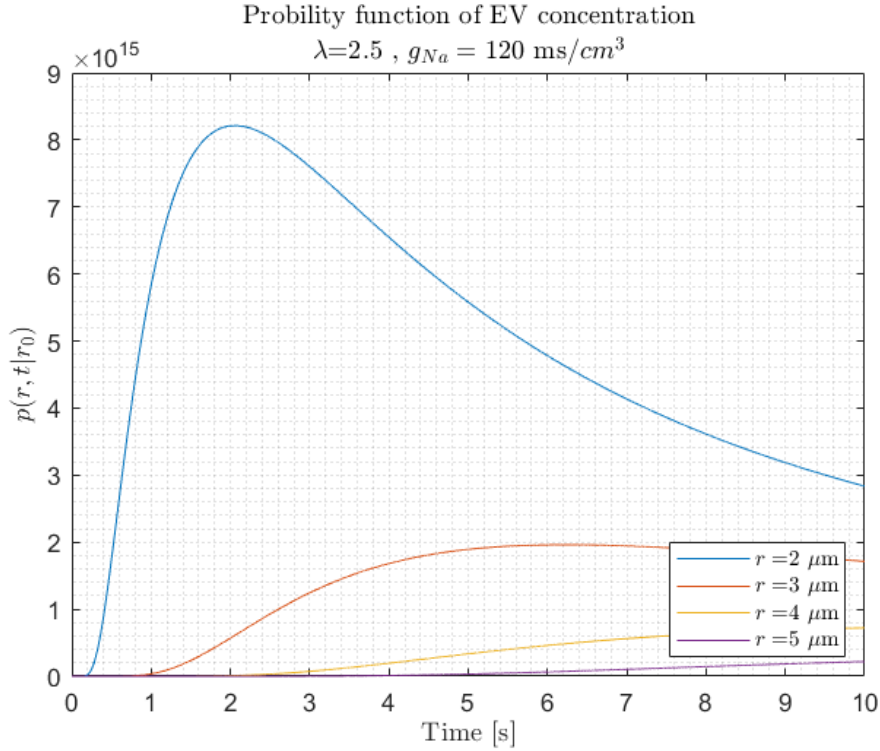


Figure 19: Probability function of EVs concentration at different r positions, unhealthy case.

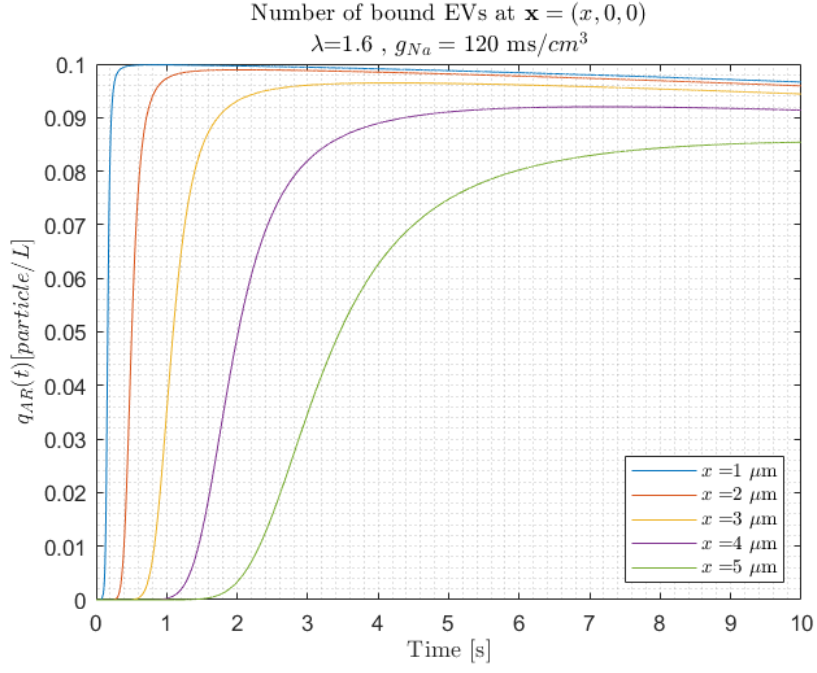
4.3 Uptake

To understand how EVs are taken up by the receiver, we simulated the uptake process and calculated the number of bound EVs and internalized EVs. The results from this section are presented in Chapter 3, as they give an overview of the performance of the end-to-end model.

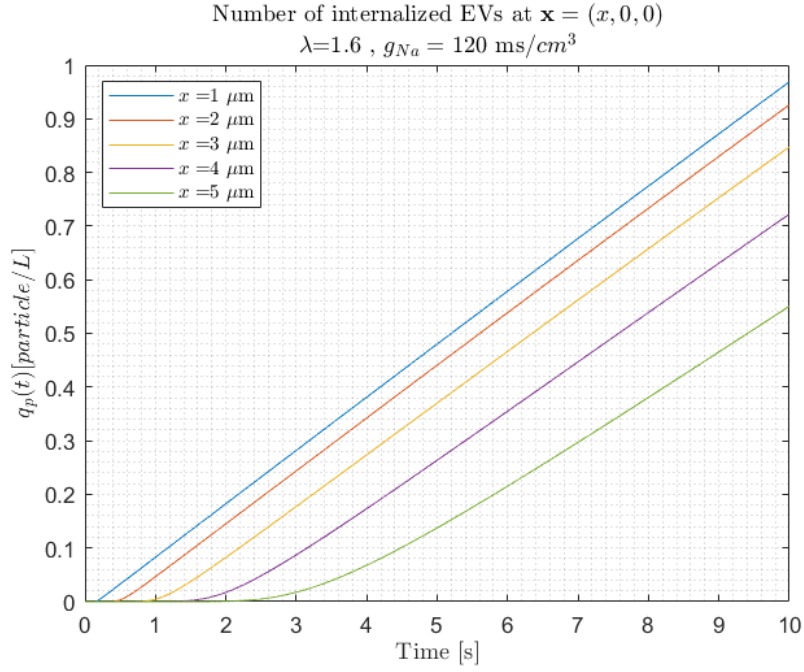
In our study, we used two different models, as discussed in Section 2.3, to simulate the uptake mechanisms. These models differed in their level of complexity and how well they accounted for the effects of the channel and its interaction with the receiving cells. For both models, the released EVs concentration from Section 4.1 was used as the input of the propagation channel.

For the diffusion-advection model, an ODE-based approach was proposed in Section 2.3.1, where the channel output from Section 4.2.1 is used as the initial value for solving the systems of ODEs. The results from this solution are presented in Section 3.1.

Solving the system of ODEs with the software ODE solver can result in negative values, which are not physically valid. So for the result presented in Section 3.1, we limited the solver to provide non-negative results. However, the MM assumption explained in Section 2.3.1 can be used as an alternative to calculate the number of bound and internalized EVs. Simulating (24) simplifies the simulation process and yields comparable results to solving the ODEs as shown in Figure 24. This confirms the validity of the MM assumption in our study. However, as mentioned in [38], the MM assumption has the limitation to be only valid when the number of binding sites is significantly fewer than the number of initial EVs. Therefore solving the ODEs directly has the potential to be used in a wider range of scenarios.



(a) Number of bound EVs from MM approach.



(b) Number of internalized EVs from MM approach.

Figure 20: Bound and internalized EVs from MM approach in (24).

To calculate the concentration of bound and internalized EVs in the PIC model, the released EV concentration from Section 4.1 is convolved with the detection probability, defined in (28). The results from this simulation are presented in Section 3.2.

4.4 End-to-end Model

The final results from the simulation of the two proposed end-to-end models are presented in Chapter 3.

The two methods are different in their level of complexity and how they model the propagation and uptake of EVs. The PIC model is based on the probabilities defined in (27) and (28). It takes into account the receiver interaction with the propagated EVs, and models the channel together with the receiving cell. This makes the calculations simpler and more straightforward. However, in the diffusion-advection model, the channel impulse response is modeled separately in (13), and the number of bound and internalized EVs shall be derived from solving a system of ODEs. This is complicated and can yield results that are not physically feasible.

Although in our simulation the velocity vector of the diffusion-advection model was assumed to be zero, the model is capable of showing the impacts of the drift, whereas in the PIC model based on the Fokker-Planck equation (16), the advection effect of the channel was not considered.

In the diffusion-advection model, the observation point is defined in the Cartesian coordinate system, which makes the calculations and visualization of the changes in EV concentration over time complicated. The PIC model uses the radial component r , for modeling the position of EVs, which simplifies the calculations and the plotting of results.

The two models have shown similar responses to AD. Changes in Na^+ conductance, with decreasing g_{Na} parameter has resulted in a lower number of received EVs in both models, whereas increasing the tortuosity parameter with increasing λ value has resulted in a delayed peak of concentration and slower movement of EVs for both models. These results suggest that the proposed methods effectively capture the characteristics of AD. Furthermore, this indicates that monitoring cell-to-cell communication performance has the potential to serve as a biomarker for early detection of AD.

5 Conclusion and Future Work

In this thesis, two methods for modeling EV-mediated cell-to-cell communication between neurons were utilized. The methods are modeling the molecular communication between the cells in the communication systems framework where the neurons act as the transceivers, and the brain ECM serves as the propagation channel. Our main focus in this research was to understand the transmission of EVs between neurons, thus their release rate, concentration in the propagation channel, and the number of taken EVs were used to determine the performance of the communication link.

The goal of this research was to understand how AD affects the molecular communications of EVs in the brain. The focus here was on the accumulation of amyloid-beta plaques and the erosion of the brain structure due to the disease. In this work, AD's impact on the transmitting neurons and the channel was modeled by modifying key parameters associated with the disease. By changing these parameters, AD's effect on the defined communication links was found to have the potential to serve as a biomarker for earlier detection and diagnosis of the disease.

Moving forward, there are ways to enhance the two developed models. In the diffusion-advection model, we can explore how adding a non-zero velocity for the ECM and observing the results in three dimensions would make the simulation more comprehensive. As for the PIC model, an important future improvement would be to include the effect of drift in the Fokker-Planck equation. This would make the model more complete in terms of modeling all impacts from the propagation channel.

Moreover, when modeling AD, we only modified two parameters in the transmitter and channel components. To make the models more comprehensive, it is suggested to investigate other important factors that may be affected during the early stages of AD. This can be achieved by collaborating with biologists and experts in the field to gain insights into additional parameters that play a role in AD progression.

Furthermore, we encountered challenges in modeling the impact of AD on the receiver, as no significant effects were observed in our research. However, this presents an opportunity for improvement. Further investigation is required to identify any changes in the receiving neurons that may occur in relation to AD. By addressing this aspect, we can enhance the accuracy and applicability of the models in capturing the complete dynamics of the disease.

The current methods focus on point-to-point communication between individual cells. However, there is potential to extend these models to a more complex scenario involving multiple transmitters and receivers. By considering a network of cells, we can study how AD affects the overall communication dynamics within the brain.

In this extended scenario, it would be valuable to model the effects of AD-related neural loss. Neural loss is a significant characteristic of AD, and including this aspect in the models would provide a more comprehensive understanding of the disease's impact on molecular communication.

References

- [1] Y. Gao and X. Liu, “Secular Trends in the Incidence of and Mortality Due to Alzheimer’s Disease and Other Forms of Dementia in China From 1990 to 2019: An Age-Period-Cohort Study and Joinpoint Analysis,” *Frontiers in Aging Neuroscience*, vol. 13, 9 2021.
- [2] Z. Breijyeh and R. Karaman, “Comprehensive Review on Alzheimer’s Disease: Causes and Treatment.” *Molecules (Basel, Switzerland)*, vol. 25, no. 24, 12 2020.
- [3] M. Gabrielli, F. Tozzi, C. Verderio, and N. Origlia, “Emerging Roles of Extracellular Vesicles in Alzheimer’s Disease: Focus on Synaptic Dysfunction and Vesicle–Neuron Interaction,” *Cells*, vol. 12, no. 1, 2023.
- [4] J. Rasmussen and H. Langerman, “Alzheimer’s Disease – Why We Need Early Diagnosis,” *Degenerative Neurological and Neuromuscular Disease*, vol. Volume 9, 2019.
- [5] S. Lee, S. Mankhong, and J. H. Kang, “Extracellular Vesicle as a Source of Alzheimer’s Biomarkers: Opportunities and Challenges,” *International Journal of Molecular Sciences*, vol. 20, no. 7, 2019.
- [6] K. G. Yiannopoulou and S. G. Papageorgiou, “Current and Future Treatments in Alzheimer Disease: An Update,” *Journal of Central Nervous System Disease*, vol. 12, 2020.
- [7] Alzheimer’s Association. (2023) Alzheimer’s association. [Online]. Available: <https://www.alz.org/help-support/i-have-alz/treatments-research>
- [8] R. Tarawneh and D. M. Holtzman, “The clinical problem of symptomatic Alzheimer disease and mild cognitive impairment,” *Cold Spring Harbor Perspectives in Medicine*, vol. 2, no. 5, 2012.
- [9] L. L. Beason-Held, J. O. Goh, Y. An, M. A. Kraut, R. J. O’Brien, L. Ferrucci, and S. M. Resnick, “Changes in brain function occur years before the onset of cognitive impairment,” *Journal of Neuroscience*, vol. 33, no. 46, 2013.
- [10] C. R. Jack, D. A. Bennett, K. Blennow, M. C. Carrillo, B. Dunn, S. B. Haeberlein, D. M. Holtzman, W. Jagust, F. Jessen, J. Karlawish, E. Liu, J. L. Molinuevo, T. Montine, C. Phelps, K. P. Rankin, C. C. Rowe, P. Scheltens, E. Siemers, H. M. Snyder, R. Sperling, C. Elliott, E. Masliah, L. Ryan, and N. Silverberg, “NIA-AA Research Framework: Toward a biological definition of Alzheimer’s disease,” *Alzheimer’s and Dementia*, vol. 14, no. 4, 2018.
- [11] J. E. Galvin, P. Aisen, J. B. Langbaum, E. Rodriguez, M. Sabbagh, R. Stefanacci, R. A. Stern, E. A. Vassey, A. de Wilde, N. West, and I. Rubino, “Early Stages of Alzheimer’s Disease: Evolving the Care Team for Optimal Patient Management,” *Frontiers in Neurology*, vol. 11, 2021.
- [12] Alzheimer’s Association. (2023) Alzheimer’s association. [Online]. Available: https://www.alz.org/alzheimers-dementia/diagnosis/medical_tests
- [13] ——. (2023) Alzheimer’s association. [Online]. Available: <https://www.alz.org/alzheimers-dementia/research-progress/earlier-diagnosis>
- [14] I. İŞIK, “Classification of Alzheimer Disease with Molecular Communication Systems using LSTM,” *International Journal of Computational and Experimental Science and Engineering*, 2022.
- [15] L. Harvey, B. Arnold, Z. S Lawrence, I. M. Pau, B. David, and D. James, “Molecular Cell Biology. 4th edition,” *Journal of the American Society for Mass Spectrometry*, 2000.
- [16] B. Alberts, “Essential cell biology: an introduction to the molecular biology of the cell,” *Biology of the Cell*, vol. 171, 1998.
- [17] Y. Moritani, S. Hiyama, and T. Suda, “Molecular Communication A Biochemically-Engineered Communication System,” in *Proceedings of the Frontiers in the Convergence of Bioscience and Information Technologies, FBIT 2007*, 2007.

-
- [18] Y. Chahibi, "Molecular communication for drug delivery systems: A survey," *Nano Communication Networks*, vol. 11, 2017.
- [19] L. Felicetti, M. Femminella, G. Reali, and P. Liò, "Applications of molecular communications to medicine: A survey," *Nano Communication Networks*, vol. 7, 2016.
- [20] H. K. Rudsari, M. Zoofaghari, M. Veletić, J. Bergsland, and I. Balasingham, "The End-to-End Molecular Communication Model of Extracellular Vesicle-based Drug Delivery," *IEEE Transactions on NanoBioscience*, pp. 1–1, 2022.
- [21] M. Lekić, M. Zoofaghari, M. Veletić, and I. Balasingham, "Extracellular vesicle propagation in acidic tumor microenvironment," in *Proceedings of the 9th ACM International Conference on Nanoscale Computing and Communication, NANOCOM 2022*, 2022.
- [22] R. Quiroz-Baez, K. Hernández-Ortega, and E. Martínez-Martínez, "Insights Into the Proteomic Profiling of Extracellular Vesicles for the Identification of Early Biomarkers of Neurodegeneration," *Frontiers in Neurology*, vol. 11, 2020.
- [23] D. M. Lovinger, "Communication Networks in the Brain," *Alcohol Research & Health*, vol. 31, no. 3, 2008.
- [24] N. Farsad, H. B. Yilmaz, A. Eckford, C. B. Chae, and W. Guo, "A comprehensive survey of recent advancements in molecular communication," *IEEE Communications Surveys and Tutorials*, vol. 18, no. 3, 2016.
- [25] L. Bongiovanni, A. Andriessen, M. Wauben, E. N. M. N. Hoen, and A. De Bruin, "Extracellular Vesicles: Novel Opportunities to Understand and Detect Neoplastic Diseases." *Veterinary Pathology*, 2021.
- [26] F. Cali, L. Fichera, and N. Tuccitto, "Comprehensive step-by-step procedure to setup a molecular communication through liquid experiment," *MethodsX*, vol. 9, 2022.
- [27] M. Sheng, B. L. Sabatini, and T. C. Südhof, "Synapses and Alzheimer's disease," *Cold Spring Harbor Perspectives in Biology*, vol. 4, no. 5, 2012.
- [28] M. Garcia-Contreras and A. S. Thakor, "Extracellular Vesicles in Alzheimer's Disease: from Pathology to Therapeutic Approaches." *Neural regeneration research*, vol. 18, no. 1, pp. 18–22, 1 2023.
- [29] H. Arjmandi, H. K. Rudsari, J. Santos, M. Zoofaghari, O. Ievglevskiy, M. Kanada, A. Khaleghi, I. Balasingham, and M. Veletic, "Extracellular Vesicle-Mediated Communication Nanonetworks: Opportunities and Challenges," *IEEE Communications Magazine*, vol. 59, no. 5, 2021.
- [30] L. G. Wu, E. Hamid, W. Shin, and H. C. Chiang, "Exocytosis and endocytosis: Modes, functions, and coupling mechanisms," *Annual Review of Physiology*, vol. 76, 2014.
- [31] M. Veletić, M. T. Barros, H. Arjmandi, S. Balasubramaniam, and I. Balasingham, "Modeling of Modulated Exosome Release From Differentiated Induced Neural Stem Cells for Targeted Drug Delivery," *IEEE Transactions on NanoBioscience*, vol. 19, no. 3, pp. 357–367, 7 2020.
- [32] J. T. Low, A. Shukla, N. Behrendorff, and P. Thorn, "Exocytosis, Dependent on Ca²⁺ Release from Ca²⁺ Stores, is Regulated by Ca²⁺ Microdomains," *Journal of Cell Science*, vol. 123, no. 18, pp. 3201–3208, 9 2010.
- [33] M. Häusser, "The hodgkin-huxley theory of the action potential," *Nature Neuroscience*, vol. 3, no. 11s, 2000.
- [34] M. Watts and A. Sherman, "Modeling the pancreatic α -cell: Dual mechanisms of glucose suppression of glucagon secretion," *Biophysical Journal*, vol. 106, no. 3, 2014.
- [35] J. T. Brown, J. Chin, S. C. Leiser, M. N. Pangalos, and A. D. Randall, "Altered Intrinsic Neuronal Excitability and Reduced Na⁺ Currents in a Mouse Model of Alzheimer's Disease," *Neurobiology of Aging*, vol. 32, no. 11, pp. 1–2109, 11 2011.
-

-
- [36] C. Perez and G. Ullah, “Reduced cooperativity of voltage-gated sodium channels in the hippocampal interneurons of an aged mouse model of Alzheimer’s disease.” *European biophysics journal : EBJ*, vol. 47, no. 5, pp. 539–547, 7 2018.
- [37] O. B. Akan, H. Ramezani, T. Khan, N. A. Abbasi, and M. Kuscu, “Fundamentals of molecular information and communication science,” *Proceedings of the IEEE*, vol. 105, no. 2, 2017.
- [38] M. Damrath, M. Zoofaghari, and M. Veletić, “Computational Estimation of Chemical Reaction Rates in Extracellular Vesicle Signaling, Nano Communication Networks,” *Nano Communication Networks*, 2023.
- [39] M. Veletić, M. Damrath, M. Zoofaghari, H. K. Rudsari, and I. Balasingham, “Capacity of Diffusive Particle Intensity Channels with Reactive Receivers,” Submitted to GLOBECOM.
- [40] E. Barbará-Morales, J. Pérez-González, K. C. Rojas-Saavedra, and V. Medina-Bañuelos, “Evaluation of Brain Tortuosity Measurement for the Automatic Multimodal Classification of Subjects with Alzheimer’s Disease,” *Computational Intelligence and Neuroscience*, vol. 2020, 2020.
- [41] E. Syková and N. Charles, “Diffusion in brain extracellular space.” *Psychological Review*, vol. 88, 2008.
- [42] A. Ahmadzadeh, H. Arjmandi, A. Burkovski, and R. Schober, “Comprehensive Reactive Receiver Modeling for Diffusive Molecular Communication Systems: Reversible Binding, Molecule Degradation, and Finite Number of Receptors,” in *IEEE Transactions on Nanobioscience*, vol. 15, no. 7, 2016.
- [43] S. V. Krylova and D. Feng, “The Machinery of Exosomes: Biogenesis, Release, and Uptake,” *International Journal of Molecular Sciences*, vol. 24, no. 2, 2023.
- [44] K. O’Brien, S. Ughetto, S. Mahjoun, A. V. Nair, and X. O. Breakefield, “Uptake, functionality, and re-release of extracellular vesicle-encapsulated cargo,” *Cell Reports*, vol. 39, no. 2, 2022.
- [45] Z. H. Kwok, C. Wang, and Y. Jin, “Extracellular vesicle transportation and uptake by recipient cells: A critical process to regulate human diseases,” *Processes*, vol. 9, no. 2, 2021.
- [46] A. Lombardo, G. Morabito, C. Panarello, and F. Pappalardo, “Modeling Biological Receivers: The Case of Extracellular Vesicle Fusion to the Plasma Membrane of the Target Cell,” in *Proceedings of the 9th ACM International Conference on Nanoscale Computing and Communication, NANOCOM 2022*, 2022.
- [47] A. L. Hodgkin and A. F. Huxley, “A quantitative description of membrane current and its application to conduction and excitation in nerve,” *The Journal of Physiology*, vol. 117, no. 4, 1952.

Appendix

| Component | Parameter | Definition | Value | Unit | Ref. |
|--------------|------------------|--|---------------|---|------|
| Release | g_K | potassium channel membrane conductance | 36 | ms/cm^3 | [47] |
| | V_K | potassium channel Nernst potential | -70 | mV | |
| | g_{Na} | sodium channel membrane conductance | 120 | ms/cm^3 | |
| | V_{Na} | sodium channel Nernst potential | 50 | mV | |
| | g_L | leak channel membrane conductance | 0.3 | ms/cm^3 | |
| | V_L | leak channel Nernst potential | -54.4 | mV | |
| | c_m | membrane capacitance | 1 | $\mu\text{F}/\text{cm}^3$ | |
| Propagation | D | diffusion coefficient | $1e^{-12}$ | m^2/s^2 | [20] |
| | λ | tortuosity | 1.6 | | [41] |
| | k_d | effective degradation | $2e^{-04}$ | s^{-1} | |
| | α | volume fraction of ECM | 0.2 | | |
| | | | | | |
| Uptake - ODE | k_b | backward(recycling) rate | 0.11 | s^{-1} | [38] |
| | k_f | forward(binding) rate | 0.13 | s^{-1} | |
| | k_i | internalization rate | 1 | s^{-1} | |
| | N | Number of binding sites | 0.1 | | |
| | | | | | |
| Uptake - PIC | k_b | backward(recycling) rate | 0.11 | s^{-1} | [38] |
| | k_f | forward(binding) rate | $3.14e^{-14}$ | $\text{particle}^{-1}\text{m}^3/\text{s}$ | [39] |
| | k_i | internalization rate | 1 | s^{-1} | [38] |
| | r_0 | release point | 1 | μm | [39] |
| | a | receiver radius | 0.5 | μm | [39] |
| | N_{ref} | reference number of particles | 0.1 | | [39] |

Table 1: Values and parameters for the simulations.



 **NTNU**

Norwegian University of
Science and Technology